energies

MDPI

*Article*

# Asymmetric Substitution and Energy Import Dependence: A Non-Linear Assessment of the Transport–Energy–Tourism Nexus in a Constraints-Driven Economy

**Wai In Ho, Yifen Yin, Yuanyuan Yu and Chunning Wang ***

Faculty of Humanities and Social Sciences, Macao Polytechnic University, Macao 999078, China
* Correspondence: p2424662@mpu.edu.mo

**Abstract**

The energy implications of transport electrification are presumed to fall on the power grid, yet the fuel and electricity margins are rarely examined in parallel, and never in a tourism-driven economy heavily dependent on imported electricity. This paper takes Macau—where approximately ninety percent of electricity is imported, supply reliability is saturated, and tourism dominates demand—as an extreme case. Using monthly data from January 2010 to July 2026, we estimate within a nonlinear autoregressive distributed lag (NARDL) framework the long-run equilibrium associations between electric vehicle (EV) penetration and two distinct dimensions, namely gasoline consumption (fuel substitution margin) and electricity import dependence (electricity margin). Bootstrap bounds testing accommodates the near-$I(2)$ character of the penetration series. The fuel margin shows a negative long-run association, with log-form point estimates spanning −0.27 to −0.62. The association is statistically firm in the full and handover windows, whereas the EV-era estimate halves to −0.27 and loses conventional significance once residual seasonality is corrected. Identification is contingent on the diffusion trend, so the range is interpreted as an upper bound on substitution rather than a magnitude attributable to electrification alone. The electricity margin shows a bounded null: eight of nine specifications yield no detectable association; the sole significant estimate is form-dependent and inconsistent with observed trends. Minimum detectable effect calculations and the observation that charging load constitutes less than 0.4% of total electricity consumption jointly bound any plausible effect. Tourism exhibits asymmetry consistent with a ratchet in the full and handover windows, where the elasticity with respect to visitor inflows (0.08–0.09) exceeds that of outflows (0.05–0.07), with the pattern attenuating under alternative specifications. In this constraints-driven tourism economy, electrification is reshaping the fuel ledger while the electricity ledger remains undisturbed.

**Keywords:** electric vehicle penetration; fuel substitution; energy import dependence; NARDL; asymmetry; tourism economy; Macau

Check for updates

Academic Editors: Lefki Papada and Dimitris Damigos

Received: 11 October 2026
Revised: 28 October 2026
Accepted: 30 October 2026
Published: 1 November 2026

**Correction Statement:** This article has been republished with a minor change. The change does not affect the scientific content of the article and further details are available within the backmatter of the website version of this article.

**Copyright:** © 2026 by the authors. Licensee MDPI, Basel, Switzerland. This article is an open access article distributed under the terms and conditions of the Creative Commons Attribution (CC BY) license.

## 1. Introduction

The electrification of transport is reshaping the demand structure of urban energy systems. Over the past decade, electric vehicles (EVs) have moved from policy pilots to mass penetration; experience across economies consistently points to their potential for reducing oil consumption and carbon emissions, while simultaneously raising concerns about whether power systems can absorb the charging load [1–3]. In the engineering

and energy economics literature, the spatiotemporal distribution of EV charging load, distribution network capacity constraints, and expansion costs constitute a mature research field [4–6], whose findings converge on the same direction: the higher the penetration rate, the greater the grid stress, and the more urgent the need for active management.

This "EV–grid stress" narrative rests on two premises that have not been adequately tested. The first concerns margin selection. Transport electrification is, first and foremost, a substitution process in which internal combustion engine displacement drives a simultaneous reduction in gasoline consumption and growth in electricity demand. Yet existing research rarely examines both margins in tandem: one strand of literature focuses on charging load and grid planning [3,5,7], while another addresses fuel substitution and life-cycle accounting [8–10]. Consequently, empirical investigations that integrate both margins into a unified econometric framework remain scarce. The second premise concerns system configuration. The grid stress literature focuses primarily on large interconnected systems, implicitly assuming that domestic generation expansion responds to load growth. In economies where electricity is overwhelmingly imported, the appropriate characterization of the electricity margin is not generation capacity but the structure of import dependence, where the core energy security challenge lies in allocating load between domestic generation and imported power [11,12].

The situation of such economies on this question is often underestimated. A constraints-driven economy—characterized by tight land availability, scarce primary energy, and bounded grid capacity—has neither the spatial room for domestic renewable deployment nor the option of absorbing new load through large-scale generation investment. When such an economy is simultaneously tourism-dominated, transport and energy demand carry the additional burden of externally driven volatility. Macau offers an extreme exemplar of this dynamic. Approximately ninety percent of its electricity is imported through the China Southern Power Grid, with local generation serving only peak-shaving and security functions. Meanwhile, supply reliability consistently ranks among the world's best, with annual average customer interruption duration measured in minutes. Furthermore, monthly visitor arrivals dominate energy load fluctuations [13,14], and EV penetration surged from under 0.3% at year-end 2019 to 7.9% by mid-2026, accompanied by a concentrated expansion of public charging infrastructure in 2022. A system with saturated reliability and both energy margins locked by external constraints provides near-laboratory conditions for examining which energy account electrification actually touches.

The literature leaves three gaps. First, the dual margins lack parallel testing: studies of EVs' energy effects fall either on the power system side or on the fuel substitution side; rarely does a single framework address both questions of how much oil is displaced and how much electricity is added [3,7,10]. Second, the asymmetric transport–energy relationship in a tourism monoculture is untested: asymmetric evidence in the tourism–energy literature concentrates on electricity and emissions [15–17]; how tourism load shapes the long-run structure of transport fuel, and whether expansion and contraction operate symmetrically, have not been examined at monthly frequency. Third, evidence of "no effect" in a high-reliability import system is absent: existing EV–grid research almost universally presumes stress exists and focuses on quantifying it [4–6]; when system reliability is saturated and charging load constitutes a negligible share, the inability to detect an effect is itself informative, yet such bounded null results are absent from the literature [11,12].

This paper uses Macau as its subject, employing monthly data from January 2010 to July 2026 within a nonlinear autoregressive distributed lag (NARDL) framework [18,19] to address two questions. First, what long-run equilibrium associations exist between EV penetration and two energy margins—the fuel margin, characterized by gasoline consump-

tion, and the electricity margin, characterized by electricity import dependence? Second, does tourism load exert asymmetric effects on transport fuel—that is, do expansion and contraction operate with equal force?

This paper makes three contributions. First, it proposes and implements a dual-margin parallel testing design. Using the same dataset and the same method to simultaneously estimate the long-run coefficients of EV penetration on the fuel and electricity margins, placing the questions of "how much is substituted" and "whether the grid is touched"—normally belonging to separate literatures—within one comparable framework. On the data side, we construct a monthly time series verified by accounting identities and three-source temperature cross-validation, with all series traceable to official primary records. Second, it provides a bounded-null protocol for zero results. For the undetected association on the electricity margin, we simultaneously report the confidence interval upper bound, the minimum detectable effect, and an order-of-magnitude calculation, rendering "no detectable effect" an assessable piece of evidence rather than a narrative claim. Third, it supplies asymmetric evidence for a tourism monoculture. Tourism load enters the long-run equation with separate positive and negative partial sums, its ratcheted character is examined, and its role is identified alongside EV penetration within the same structure.

## 2. Background and Literature Review

### *2.1. The Macau Energy and Transport System*

Macau's power system exhibits an "import-dominated, locally peak-shaved" configuration. Approximately ninety percent of electricity is imported from the China Southern Power Grid, while local generation, primarily comprising oil-fired and natural gas units, serves peak-shaving, standby, and supply security functions [20]. Cross-border electricity trade operates under long-term contracts whose purchase prices are proprietary. Alongside its heavy reliance on imported power, the local grid maintains exceptionally high reliability; Macau's grid consistently ranks among the world's most reliable, with annual average customer interruption duration measured in minutes. Consequently, the macro energy ledger is externally anchored. Primary energy is almost entirely imported, transport fuels consist predominantly of gasoline and light diesel, and local electricity generation remains contingent on imported fuels and external power. Life-cycle greenhouse gas accounting shows that energy import and conversion constitute the primary sources of Macau's urban emissions [20].

Transport electrification began late but subsequently expanded at a rapid pace. Macau has exempted qualifying electric vehicles from motor vehicle tax since 2012, yet EV penetration remained below 0.3% through the end of 2019. After 2020, adoption accelerated markedly, reaching approximately 7.9% by mid-2026. Concurrently, charging infrastructure expanded in a policy-driven, pulsed pattern, with public charging points surging from 170 at end-2021 to approximately 1530 at end-2022, then climbing moderately to approximately 2300 by March 2026. This "initially sparse, then pulsed" infrastructure supply trajectory provides leverage for distinguishing demand-side from supply-side effects of electrification.

The dominant demand-side force is tourism. Macau represents a quintessential tourism monoculture, where monthly visitor arrivals exhibit substantial volatility that surpasses most domestic socioeconomic indicators. Consequently, gaming, hospitality, and cross-border transport constitute the primary marginal drivers of energy load [13,14]. The transport–energy–tourism nexus has received growing scholarly attention. Specifically, wavelet analysis shows that motor vehicle ownership is significantly positively correlated with gasoline and light diesel consumption [13], while a structural vector autoregression study finds that economic policy uncertainty shocks transmit to energy consumption through the tourism sector [14]. These studies confirm the tight coupling of transport,

energy, and tourism in Macau, but neither addresses electrification—the force currently reshaping the transport energy structure.

### *2.2. Electric Vehicles and Power Systems: From Load Shock to Capacity Planning*

Research on EV–power system interactions has developed along a "load characterization →impact assessment→planning response" trajectory. Early work established statistical models of charging load [4], which were subsequently extended to evaluate distribution network voltage, transformer loading, and expansion requirements under varying penetration scenarios [5–7]. Data-driven methods and open data have further improved estimates of the spatiotemporal distribution of charging demands [21,22]. Assessments of systems such as the UK consistently find that uncontrolled charging at higher penetration imposes substantial distribution network stress, while controlled charging and intelligent scheduling significantly mitigate impacts [5,7,21]. At a broader level, the effect of EV deployment on generation structure and emissions depends on the cleanliness of the electricity mix [10,23], and vehicle-to-grid (V2G) interaction is considered to have peak-shaving and system value, though its economic feasibility is constrained by user participation willingness [24].

Specifically, Suski et al. [1] simulated EV load impacts on the grid using the Maldives as a case study, finding that uncontrolled charging at 20% penetration could trigger distribution voltage violations, a threshold that substantially exceeds empirical levels in most emerging markets. Nogueira et al. [2] analyzed 2030 scenarios for the Portuguese distribution network, showing that transformer overload risk rises significantly when EV penetration exceeds 30%. Alquthami et al. [3] similarly found in Saudi system simulations that spatiotemporal charging concentration represents the primary source of grid stress, which intelligent scheduling can substantially alleviate. Rautiainen et al. [4] established a statistical charging load model based on Finnish travel survey data, laying the methodological foundation for subsequent research. Crucially, these studies share the implicit premise that the power system is dominated by domestic generation and that load growth necessitates a domestic capacity expansion response. Macau-specific evidence on the energy-system side exists but stops short of EV–grid interaction: urban energy accounting attributes the territory's emissions primarily to energy import and conversion [20], the well-to-wheel assessment of light-duty electrification shows that its greenhouse-gas consequences hinge on the externally anchored generation mix [25], and distribution-level hosting-capacity and reliability frameworks sharpen the engineering side of the question without Macau calibration [26,27]. To our knowledge, no published study has estimated how EV penetration interacts with Macau's power system at the macro level; the electricity margin of this paper addresses precisely this vacancy.

On the energy security and import dependence dimension, the existing literature approaches the problem from two angles. The first is energy transition research on small island developing states. Gay et al. [11] noted that small-capacity systems have thin spinning reserves and limited frequency regulation resources, making EV integration constraints fundamentally different from continental systems; V2G may actually carry relatively greater system value in small systems. Edoo and King [12] planned a 100% renewable energy scenario for Mauritius, treating transport electrification as a demand-side resource for balancing domestic renewable output. The second is the general energy import dependence literature, which focuses on energy security gains from import diversification, macroeconomic costs of import disruption, and the interaction between import contract structures and domestic dispatch. However, no study has formally examined EV penetration as a potential disturbance source for import dependence structure. This paper's electricity margin test fills this gap precisely: in an economy where ninety percent of electricity comes from a

single contractual source, whether and how EV penetration alters the import dependence structure has not been formally tested.

This literature stream predominantly reflects the characteristics of large, self-sufficient interconnected systems, leaving small, import-dependent grids underrepresented, and for a system like Macau's—import-dominated with saturated reliability—prior research has neither posed nor tested the question of whether EV penetration observably shifts import dependence structure when local generation serves only peak-shaving and charging load constitutes less than one percent of total consumption.

### 2.3. Electric Vehicles and Transport Fuel Substitution

The body of research on the fuel margin is far smaller than on the electricity margin, and methods fall into two categories. The first is based on measurement and simulation, comparing per-kilometer energy consumption between electric and conventional vehicles [8], fleet-level impacts of electrification on on-road energy use [10], and full-cycle energy and emission differences among hybrid, plug-in hybrid, and battery electric vehicles [9]. Macau-specific life-cycle assessment also shows that light-duty vehicle electrification carries greenhouse gas reduction potential contingent on the electricity mix [25]. The second category uses econometric models to examine drivers of EV market penetration—subsidies and costs [28], cross-country structural differences in sales [29], actual utilization of driving range [30]—and macro-level assessments of electrification's effects on energy consumption and emissions [23]. Relevant case studies offer empirical benchmarks; for instance, Beijing's electrification transition involved concurrent restructurings of fleet composition and urban energy consumption [31], while Singapore's cost-effectiveness analysis evaluated electrification under city-state constraints [32].

Regarding substitution elasticity magnitudes, existing research provides comparable benchmarks. Wang et al. [8], based on real-world Beijing driving cycle data, showed that per-kilometer energy consumption of EVs is approximately 30–40% that of comparable conventional vehicles, corresponding to a per-vehicle fuel saving ratio of roughly 60–70% under one-for-one substitution (the residual share reflecting EV electricity use, part of it locally generated). This ratio is a vehicle-level benchmark of substitution intensity, not a penetration elasticity: the elasticity estimated in this paper measures the proportional gasoline decline associated with a proportional rise in fleet penetration, and the two are linked only through fleet-composition arithmetic (share-to-log-point translation, as in Section 5.2). Wang et al. [9] extended this ratio to include the generation stage in a China life-cycle assessment, concluding that net oil displacement from electrification depends on the electricity mix's cleanliness. Focusing on Macau's light-duty vehicle fleet, Song et al. [25] found significant yet mix-constrained emissions reduction potential, underscoring that when power generation structures remain externally anchored, emissions benefits depend primarily on the displacement of transport fuels. Shi et al. [31] observed in Beijing's taxi fleet that policy-driven fleet turnover induced gasoline reductions that exceeded standard one-for-one projections, driven by simultaneous efficiency gains and structural adjustments in vehicle travel.

Although these studies provide consistent directional expectations for fuel substitution, two critical limitations persist. First, substitution elasticities are rarely estimated within a dynamic cointegration framework. Because most existing work relies on cross-sectional variations or static accounting scenarios, it falls short of quantifying the long-run marginal response of fuel consumption to increases in EV penetration. Second, potential nonlinearities and asymmetries in the substitution process remain largely unexamined, particularly regarding whether gasoline demand responds symmetrically across adoption phases and how confounding macro drivers—such as tourism surges—might bias elasticity estimates.

### 2.4. Tourism–Energy Relationships and Asymmetric Evidence

The empirical literature on tourism–energy–environment relationships is vast; this paper focuses on the asymmetric strand. Panel and spatial econometric studies have established positive associations between tourism development and energy consumption and carbon emissions [15,16,33,34]. Building on this, the nonlinear autoregressive distributed lag (NARDL) model [18,19] has been widely applied to test differential transmission of positive versus negative shocks. The effects of tourism expansion and contraction on ecological footprint [16], carbon emissions [15,17], and energy consumption [35] are asymmetric in most studies, with expansion-side long-run coefficients typically exceeding contraction-side absolute values.

On the direction of asymmetry, the literature exhibits a highly consistent pattern. Lee et al. [15], using NARDL on Chinese provincial data, found that the long-run elasticity of tourism expansion on carbon emissions (0.42) exceeds the contraction-side absolute value (0.28), attributing the asymmetry to sunk costs in tourism infrastructure. Khoi et al. [16], applying asymmetric ARDL to Singapore, similarly found that tourism development's expansion-side effect on ecological footprint exceeds the contraction side. Chishti et al. [17] for South Asia, Uzuner et al. [36] for Turkey, and Wangzhou et al. [37] for Asia all report similar asymmetric patterns. Comparable asymmetries emerge on the energy demand side, where investigations of Indian oil product prices [38], Cameroonian kerosene consumption [39], and Indian industrial electricity [40] consistently document significantly different demand responses to price increases versus decreases. These findings collectively point to a behavioral economics intuition in which sunk costs associated with capacity expansion make demand easier to raise than to lower, while price asymmetries further amplify this ratchet effect.

In the Macau context, Xu and Sharif's [13] wavelet coherence analysis provides a relevant benchmark by confirming significant positive correlations between motor vehicle ownership and gasoline and diesel consumption, but wavelet methods cannot distinguish differential impacts of positive versus negative changes—precisely the advantage of NARDL partial sum decomposition. Zhang and Tian's [14] structural vector autoregression approached from the economic policy uncertainty angle, finding that EPU shocks transmit to energy consumption through the tourism sector. Both studies used total energy consumption as the dependent variable; this paper refines it to gasoline—a transport fuel subcategory—and overlays electrification's substitution effect.

In summary, the three literature streams converge on a clearly defined research gap in Macau. The electricity margin literature presumes grid stress and provides capacity planning tools, yet has not been tested in an import-dependent system. The fuel margin literature provides directional expectations but lacks elasticity estimates within a cointegration framework. The tourism-energy literature provides asymmetric methods and neighboring evidence but has not addressed the joint role of transport fuel and electrification.

### 2.5. Analytical Framework and Hypotheses

The analytical framework decomposes the energy effects of transport electrification into two margins. On the fuel margin, the displacement of internal combustion vehicles by EVs reduces gasoline consumption, where greater market penetration yields larger substitution effects. Simultaneously, tourism load enters the equation as a common driver of transport fuel, with positive and negative changes allowed different long-run coefficients. On the electricity margin, EV charging expands electricity demand, but in an import-dominated system, the marginal destination of this demand depends on its relative scale and dispatch structure—if charging load is negligible relative to system totals, or is absorbed by local

peak-shaving units and demand volatility, the import dependence structure undergoes no observable change.

Three testable hypotheses follow. H1: A long-run negative equilibrium association exists between EV penetration and gasoline consumption. H2: No detectable long-run equilibrium association exists between EV penetration and electricity import dependence; if one exists, its magnitude is constrained by the order of magnitude of charging load share. H3: Tourism load exerts asymmetric long-run effects on gasoline consumption, with the expansion-side coefficient exceeding the contraction side. All three hypotheses are stated in terms of cointegration associations.

## 3. Methodology and Data

### *3.1. Data Sources and Quality Control*

This paper constructs a monthly time series spanning January 2010 through July 2026 (199 months), with all series derived from official sources and traceable to primary records. Energy and price series come from the Macau Statistics and Census Service (DSEC) official database, including electricity consumption, electricity imports, local generation, gasoline and light diesel consumption, and retail prices for both fuels. Visitor arrivals and hotel occupancy rates are also from DSEC. Monthly gross gaming revenue is from the Gaming Inspection and Coordination Bureau (DICJ). Monthly charging point stock is from the Transport Bureau via the open data platform. Vehicle stock and new registration series are classified by use and fuel type, satisfying the fleet accounting identity—verified across all 199 months with zero residual—which simultaneously ensures the consistency of electric vehicle counts as a nested subset within vehicle families.

Monthly temperature is assembled from three sources: post-2019 data from the DSEC database; 108 months from January 2010 through December 2018 as our supplementary collection, of which May 2013 onward is extracted from Macao Meteorological and Geophysical Bureau (SMG) monthly climate reports, and January 2010 through April 2013 from the Bureau's online meteorological data query system. The three sources are cross-validated: the two supplementary sources agree exactly across 7 overlapping months; the annual means of the spliced series deviate from official annual series by no more than 0.05 °C across 9 years. To ensure data integrity, several methodological protocols were enforced: distinguishing true zeroes from missing values, generating all derived indicators programmatically from primary series, and documenting data pipelines to support complete computational reproducibility.

### *3.2. Variable Definitions, Measurement Distinctions, and Statistical Properties*

Two dependent variables are employed. The fuel margin is measured by the logarithm of gasoline consumption, $\mathrm{lng}_t$. The electricity margin is measured by electricity import dependence, $\mathrm{imp}_t = E_t^I/(E_t^I + E_t^G)$, where $E_t^I$ is imported electricity and $E_t^G$ is local generation in month $t$. It should be noted that $\mathrm{imp}_t$ is a dispatch ratio under the DSEC measurement framework, distinct from the "China Southern Power Grid supply as approximately ninety percent of total electricity consumption" whole-economy measure; the former includes local generation in the denominator, while the latter encompasses a broader supply scope with losses. All inference in this paper uses the former, with the magnitude implications of the latter examined in robustness checks.

The key explanatory variable is EV penetration rate, $\mathrm{ev}_t$, defined as the percentage share of registered electric vehicles in the total motor vehicle fleet at period end. The numerator aggregates all registered electric vehicles, namely light and heavy electric passenger cars together with light and heavy electric motorcycles: by mid-2026, electric cars constitute roughly nine percent of the car fleet and electric motorcycles roughly seven percent of

the motorcycle fleet, the latter expanded largely through the old-motorcycle replacement subsidy scheme. The two classes carry different margin implications, since motorcycles displace gasoline two-wheelers directly within a shrinking fleet and charge predominantly at residences, whereas cars add demand within a growing fleet and use public fast charging more intensively; class composition is therefore kept in view throughout (the charging-load accounting of Section 4.4 separates the two classes, and Section 4.6 reports a car-only penetration check). Given the series' accelerating diffusion pattern, both level and logarithmic forms $\ln(1 + ev_t)$ are used and reported side by side. Furthermore, the model incorporates two asymmetric regressors, namely the logarithm of retail fuel prices (gasoline for the fuel margin and light diesel for the electricity margin) and the logarithm of visitor arrivals, each decomposed into positive and negative partial sums. Temperature (°C) and monthly dummy variables serve as controls. Table 1 summarizes variable definitions, frequency, and sources.

**Table 1.** Variable definitions and sources.

| Variable | Definition | Frequency & Period | Source |
|---|---|---|---|
| $\ln g$ | Log of gasoline consumption ($10^3$ L) | Monthly, January 2010–July 2026 | DSEC Energy Statistics |
| imp | Imported electricity/(imports + local generation) | Monthly, same | DSEC Energy Statistics |
| ev | EV penetration (%): EV stock/total fleet | Monthly, same | DSEC Transport Statistics |
| $\ln p_g/\ln p_d$ | Log of gasoline/diesel retail price (MOP/L) | Monthly, same | DSEC Energy Statistics |
| $\ln v$ | Log of visitor arrivals (persons) | Monthly, same | DSEC Tourism Statistics |
| temp | Monthly mean temperature (°C), three-source spliced | Monthly, same | DSEC/SMG |
| charge | Public charging point stock (units), for robustness | Monthly, January 2019–March 2026 | Transport Bureau Open Data |
| ln ggr | Log of gross gaming revenue (MOP $10^6$), for robustness | Monthly, January 2010–July 2026 | DICJ |
| renew | Cumulative post-2010 ICE new registrations/fleet (%), for robustness | Monthly, January 2010–July 2026 | DSEC Transport Statistics |

Notes: All series verified by official accounting identities or annual anchors. Temperature splicing details in Section 3.1. $n = 199$.

Table 2 reports unit root tests. The ADF test shows that ln$g$, prices, and temperature are $I(1)$; imp and full-sample ln$v$ are I(0), satisfying the ARDL framework's mixed-order requirement. Both forms of EV penetration exhibit characteristics indicative of orders beyond $I(1)$ across both sample windows, as both the levels and first differences fail stationarity requirements under ADF and KPSS tests [41] (full-sample KPSS statistics of 1.623 and 1.702, both exceeding the 5% critical value of 0.463). Because EV diffusion is intrinsically characterized by a strong secular trend, identification primarily captures this structural movement; de-trending markedly alters coefficient magnitudes (as detailed in Section 4.6). To address the methodological challenges posed by this near-I(2) property, we report results using both level and logarithmic specifications, eschew standard asymptotic critical values in favor of bootstrap bounds testing, and interpret the resulting long-run coefficients as trend-conditioned associations. Additionally, while the ADF test classifies imp as I(0), the full-sample KPSS test rejects stationarity at the 5% level (statistic 0.705), although both tests uniformly confirm stationarity within the EV-era subsample (statistic 0.060). Given that the bounds testing framework robustly accommodates mixed I(0) and I(1) integrations,

these borderline properties are fully accounted for in the empirical modeling. Because intercept-only ADF regressions cannot separate $I(2)$ behaviour from stationarity around a deterministic trend, the last two columns of Table 2 report trend-augmented tests for both EV forms: the trend-inclusive ADF never rejects the unit root ($p \geq 0.129$ across windows and forms), and the $KPSS_\tau$ statistic rejects trend-stationarity everywhere ($p \leq 0.01$), indicating that the diffusion path behaves as a stochastic rather than a deterministic trend and supporting the near-$I(2)$ characterisation used in inference.

**Table 2.** Unit root tests (ADF and KPSS).

| Series | Window | ADF $p$ (Level) | ADF $p$ ($\Delta$) | ADF Verdict | KPSS $\eta$ (Level) | KPSS Verdict (5%) | ADF $p$ (Level, Trend) | $KPSS_\tau$ $p$ (Level, Trend) |
|---|---|---|---|---|---|---|---|---|
| $\ln g$ | W0 | 0.740 | 0.000 | $I(1)$ | 0.496 | Reject stationarity | 0.944 | — |
| $\ln g$ | W2 | 0.062 | 0.006 | $I(1)$ | 1.019 | Reject stationarity | 0.000 | — |
| imp | W0 | 0.000 | 0.000 | $I(0)$ | 0.705 | Reject stationarity | 0.000 | — |
| imp | W2 | 0.000 | 0.000 | $I(0)$ | 0.060 | Fail to reject | 0.000 | — |
| ev | W0 | 0.999 | 1.000 | $I(2)$ | 1.405 | Reject stationarity | 1.000 | ≤0.01 |
| ev | W2 | 1.000 | 0.987 | $I(2)$ | 1.522 | Reject stationarity | 1.000 | ≤0.01 |
| $\ln(1 + \text{ev})$ | W0 | 0.979 | 0.886 | $I(2)$ | 1.667 | Reject stationarity | 0.956 | ≤0.01 |
| $\ln(1 + \text{ev})$ | W2 | 0.990 | 0.086 | $I(2)$ | 1.613 | Reject stationarity | 0.129 | ≤0.01 |
| $\ln p_g$ | W0 | 0.645 | 0.000 | $I(1)$ | — | — | 0.653 | — |
| $\ln p_g$ | W2 | 0.444 | 0.000 | $I(1)$ | — | — | 0.299 | — |
| $\ln v$ | W0 | 0.008 | 0.000 | $I(0)$ | — | — | 0.039 | — |
| $\ln v$ | W2 | 0.059 | 0.000 | $I(1)$ | — | — | 0.040 | — |
| temp | W0 | 0.282 | 0.000 | $I(1)$ | — | — | 0.051 | — |
| temp | W2 | 0.162 | 0.000 | $I(1)$ | — | — | 0.678 | — |

Notes: W0 = full sample (January 2010–July 2026); W2 = EV era (January 2019–July 2026). The subsample window (January 2010–December 2024) yields conclusions consistent with W0 (magnitudes in Appendix A, Table A1). ADF specifications include an intercept, with lag selection determined by AIC (max 12). KPSS reports level form with an intercept; 5% critical value is 0.463. $p$-values and test statistics are obtained directly from test output. "—" indicates the series was not included in KPSS cross-validation, which centered on EV series and both dependent variables. The trend columns augment the deterministic terms: the ADF adds a linear trend, and the $KPSS_\tau$ statistic tests stationarity around a deterministic trend (5% critical value 0.216; "≤0.01" denotes the lower bound of the KPSS $p$-value); rejection for both EV forms in every window indicates a stochastic rather than deterministic trend.

The empirical analysis employs three distinct sample windows, encompassing the full sample W0 (January 2010–July 2026, $n = 199$, used for primary baseline estimation), an handover window W1 (January 2010–December 2024, $n = 180$), and EV era W2 (January 2019–July 2026, $n = 91$). W1 ensures comparability across earlier administrative benchmarks, while W2 captures the steep adoption phase. After accounting for lag structure and monthly dummy adjustments, effective sample sizes are 192, 173, and 84, respectively.

### *3.3. NARDL Model Specification and Inference*

We employ the nonlinear autoregressive distributed lag model [18,19]. For each asymmetric explanatory variable $x$, the positive and negative partial sum decomposition is:

$$x_t = x_0 + x_t^+ + x_t^-, x_t^+ = \sum_{i=1}^{t} max(\Delta x_i, 0), x_t^- = \sum_{i=1}^{t} min(\Delta x_i, 0) \quad (1)$$

The error correction representation is:

$$\Delta y_t = \alpha + \rho y_{t-1} + \theta' x_{t-1} + \sum_{i=1}^{p} \gamma_i \Delta y_{t-i} + \sum_{j=0}^{q-1} \pi_j' \Delta x_{t-j} + \sum_{m=2}^{12} \delta_m M_{m,t} + \varepsilon_t \quad (2)$$

where $y$ is the dependent variable, $x$ is the vector of level-entered explanatory variables (EV penetration enters symmetrically; prices and visitor arrivals are decomposed into positive and negative partial sums), and $M_m$ are monthly dummy variables. EV penetration is not subject to partial sum decomposition because it rises nearly monotonically over the sample period, leaving the negative partial sum without identifying variation. Long-run equilibrium coefficients are given by:

$$\beta = -\theta/\rho \quad (3)$$

with standard errors calculated via the delta method. Inference assumes weak exogeneity of the regressors, supported by the institutional features of the study setting. EV penetration is shaped primarily by policy pulses (such as vehicle tax exemptions and infrastructure deployments) and macroeconomic cost trends, rendering it unlikely to respond endogenously to high-frequency monthly gasoline demand shocks. Similarly, international oil prices and visitor inflows represent external market conditions facing a small open economy. Directional evidence supports this assumption for the tourism regressor: Granger-causality tests on the first-differenced pair at twelve lags reject non-causality from visitor arrivals to gasoline consumption in the full sample ($p < 0.001$) while failing to reject the reverse direction ($p = 0.191$), consistent with one-way precedence from external tourism flows to the local fuel market; in the shorter EV-era window neither direction is significant ($p = 0.128$ and 0.430), so the full-sample evidence carries the weight. As a complementary check, replacing visitor arrivals with gross gaming revenue leaves the conclusions intact (see Section 4.6). Granger precedence is evidence about temporal ordering rather than a full identification proof, and the assumption is accordingly listed among the limitations (Section 5.5).

Long-run asymmetry is tested via the Wald restriction $\theta^+ = \theta^-$. Cointegration testing employs the bounds $F$ test [19], a Wald test of the joint null that all level-term coefficients ($\rho$ and $\theta$) equal zero. Given the near-$I(2)$ character of EV penetration and monthly sample sizes, asymptotic critical values are not used; instead, the null distribution is constructed via a fixed-initial-condition residual bootstrap (1999 replications): under the restricted model with all level terms set to zero, residuals are resampled, dependent variable paths are reconstructed, and the full ECM is re-estimated with the same lag structure, yielding empirical distributions of the $F$ statistic and the ECT $t$ statistic. Bootstrap standard errors are reported to characterize Monte Carlo noise; boot $p$-values in the 0.04–0.07 range are classified as "marginal" rather than "established." The procedure is tailored to the integration properties that standard tables cannot accommodate: because the null distribution is built from the restricted model's own residuals and the reconstructed dependent-variable paths retain the stochastic trend of the observed regressors, the resulting critical values are specific to the near-$I(2)$ environment [19]. Reliability of the long-run estimates rests on three mutually reinforcing checks: the binomial Monte Carlo standard error of every boot $p$-value is reported and remains well below the decision thresholds; the estimates are invariant to the lag-selection protocol (Table A2); and they survive detrending and seasonal corrections wherever the diagnostics require such corrections (see Section 4.6 and Table A3), so inferential weaknesses would have to co-occur across all three dimensions to overturn the qualitative conclusions.

The bootstrap critical values are constructed as follows. First, we estimate the restricted model containing only differenced terms and monthly dummies (all level-term coefficients constrained to zero), obtaining residuals and fitted values. Second, we draw residuals with replacement from the restricted model, add them to fitted values to generate bootstrap

differenced dependent variable sequences, and rebuild complete dependent variable paths by cumulating from the initial period's actual value—this construction ensures the data generating process satisfies the no-cointegration null. Third, for each bootstrap path we re-estimate the full ECM using the same lag structure, compute the $F$ statistic and ECT $t$ statistic, and repeat 1999 times to form the empirical null distribution. This method's advantage lies in not relying on the Pesaran–Shin–Smith asymptotic table's $I(1)$ boundary assumption, providing direct adaptability to the near-$I(2)$ character of EV penetration. It should be noted that the reconstruction of the dependent variable path in the null distribution uses a non-recursive construction (differenced terms taken directly from restricted model fits rather than recursive feedback), which is a consistent approximation when residual autocorrelation is weak; the Monte Carlo standard error of 1999 replications is approximately 0.005–0.008.

### *3.4. Lag Selection Protocol, Diagnostics, and Robustness Design*

Model lag structures are evaluated across three distinct specifications. The baseline protocol selects optimal lag lengths via the Akaike Information Criterion (AIC) within a grid bounded by $p \leq 3$ and $q \leq 3$, while the relaxed protocol extends the search grid to $p \leq 4$ and $q \leq 4$. The fixed protocol retains the baseline lag selections to facilitate direct comparisons. Evaluating multiple lag protocols addresses empirical trade-offs in finite samples, where expanded search grids risk over-parameterization that diminishes the power of bounds and asymmetry tests, even as core point estimates remain stable. Full comparisons of all key statistics across protocols appear in Section 4.6.

Diagnostics include Breusch–Godfrey serial correlation tests (lags 1 and 12), Jarque–Bera normality, ARCH tests, and CUSUM stability tests based on recursive residuals. The electricity margin equation exhibits residual seasonal correlation at lag 12 in the EV-era window; seasonal autoregressive augmentation (adding $\Delta y_{t-12}$) does not eliminate it in those electricity-margin equations, so inference for them uses Newey–West heteroskedasticity and autocorrelation consistent (HAC) covariance [42] (lag 12) for verification, with normality deviations covered by bootstrap inference. Where the diagnostics instead require the correction, it is adopted as the primary treatment: the EV-era temperature-augmented fuel equation exhibits residual seasonality at lag 12 (Breusch–Godfrey $p = 0.012$) that the seasonal augmentation removes ($p = 0.244$), so the corrected specification carries that equation's primary estimates (Sections 4.2–4.6), with its short-sample cost of absorbed variation and wider standard errors reported alongside. Robustness checks cover: pandemic step dummies (February–June 2020, and a long version through December 2022), charging point stock entering logarithmically (2019-onward subsample), gross gaming revenue replacing visitor arrivals, asinh and common logarithm transformations of EV penetration, and the "Macau Vehicle Northbound" policy break dummy (January 2023), together with a fleet-renewal control capturing cumulative ICE registrations and a car-only EV penetration variant (Section 4.6).

## 4. Empirical Results

### *4.1. Data Overview*

Figure 1 presents the four core series. Gasoline consumption peaked in early 2019 and has trended downward since; the 2024 level is approximately twenty percent below the 2019 average. EV penetration was near zero before 2019, then followed an accelerating path to 7.9% by July 2026—the two series display clear inverse co-movement in the EV-era window. Electricity import dependence has remained in a high band of 0.58–0.96, fluctuating around a slow trend with no structural shift coinciding with EV penetration. The pandemic collapse and recovery of visitor arrivals constitutes the largest demand shock in the sample, dwarfing all other series in amplitude. The visual contrast presages this paper's core question: the

descent of gasoline and the ascent of EV penetration are temporally coupled, while import dependence shows no visible association with either—an intuition that requires formal testing within a cointegration framework.

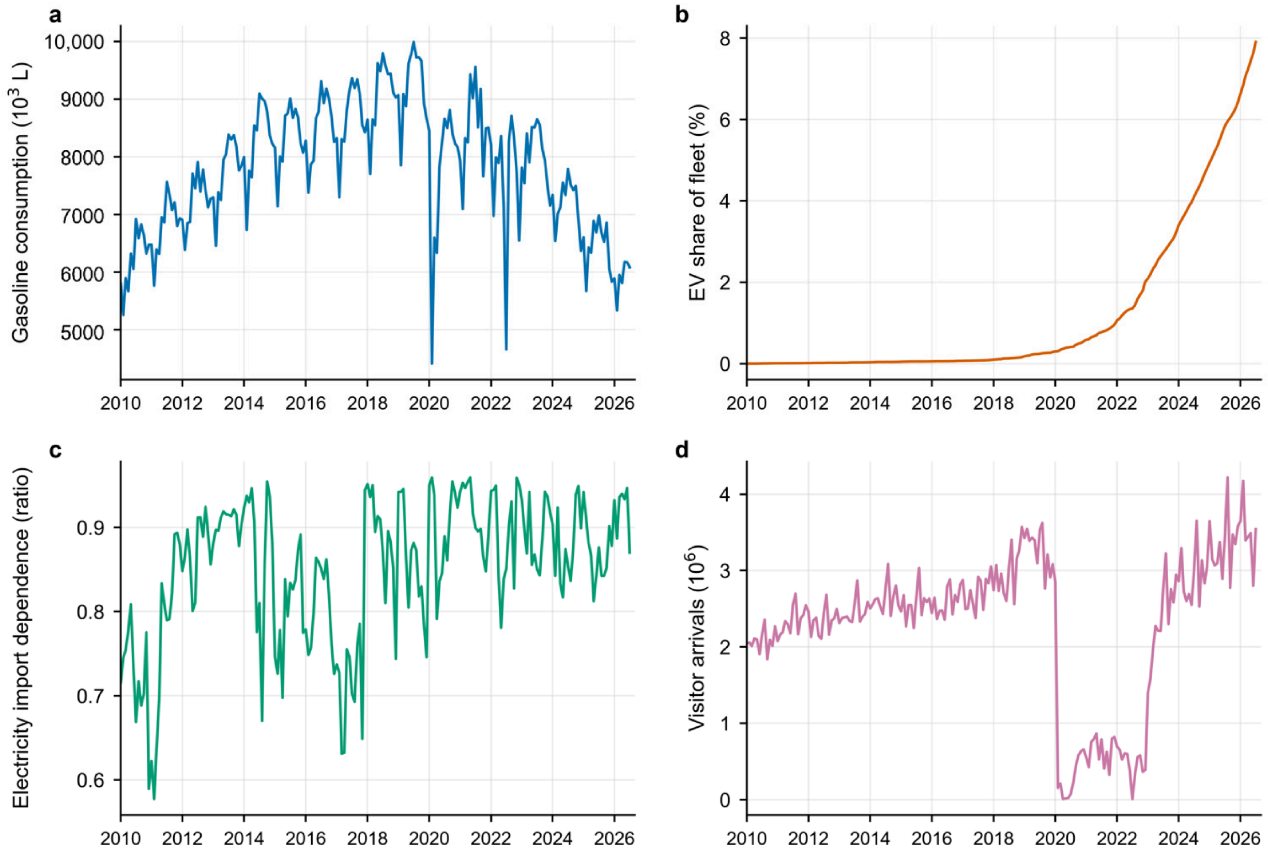


**Figure 1.** Trends in transport fuel demand, EV adoption, power import dependence, and tourism inflows (2010–2026). (**a**) Monthly gasoline consumption ($10^3$ L); (**b**) EV share of the motor vehicle fleet (%); (**c**) electricity import dependence ratio; (**d**) visitor arrivals ($10^6$ persons).

### *4.2. Cointegration Tests and Error Correction*

Table 3 reports bounds tests and error correction terms for the level and log forms of both margins. For the fuel margin (Model A), the log-form $F$-statistics across the three sample windows are 5.15, 4.97, and 8.88, with bootstrap $p$-values of 0.044 (Monte Carlo SE 0.005) for the full sample and 0.054 for the W1 window; the EV-era temperature-augmented specification yields $p < 0.001$, and its seasonally corrected counterpart remains firmly cointegrated ($F = 7.93$, $p < 0.001$), so the EV-era cointegration evidence holds on diagnostic grounds. Error correction terms are uniformly negative, and significant in all electricity-margin specifications and in the fuel-margin log forms; the full-sample log-form adjustment coefficient of −0.503 implies that approximately half of any deviation from long-run equilibrium is corrected within one month (noting that three $|\rho| > 1$ EV-era specifications exhibit oscillatory convergence with overshooting, and that the seasonally corrected EV-era $t$ ratio is weaker, $p = 0.620$, leaving the joint $F$ statistic to carry the cointegration evidence there). The level form falls into the inconclusive zone in the full sample and EV era ($p = 0.117$ and 0.156). For the electricity margin (Model B), bounds $F$ exceeds the 5% critical value in all nine specifications across three windows; however, given that import dependence is an $I(0)$ series, the $F$ rejection may partly reflect the mechanical significance of the error correction term itself (a degenerate case), and the more appropriate characterization is that Model B

equations exhibit significant error correction mechanisms, with long-run coefficient point estimates and intervals as the inferential focus.

**Table 3.** Bounds tests and error correction terms.

| Model | EV Form | Window | $F$ | Boot $p$ (MC SE) | $\rho$ (ECT) | ECT $t$ Boot $p$ | Verdict |
|---|---|---|---|---|---|---|---|
| A Fuel | Level | W0 | 4.27 | 0.117 (0.007) | −0.335 | 0.206 | Inconclusive |
| A Fuel | Log | W0 | 5.15 | 0.044 (0.005) | −0.503 | 0.020 | Marginal |
| A Fuel | Log + Temp | W0 | 4.46 | 0.049 (0.005) | −0.493 | 0.024 | Marginal |
| B Elec. | Level | W0 | 4.72 | 0.024 (0.003) | −0.326 | 0.002 | Marginal |
| B Elec. | Log | W0 | 4.78 | 0.017 (0.003) | −0.330 | 0.002 | Marginal |
| B Elec. | Log + Temp | W0 | 4.08 | 0.026 (0.004) | −0.329 | 0.003 | Marginal |
| A Fuel | Level | W1 | 4.18 | 0.112 (0.007) | −0.355 | 0.145 | Inconclusive |
| A Fuel | Log | W1 | 4.97 | 0.054 (0.005) | −0.483 | 0.030 | Marginal |
| A Fuel | Log + Temp | W1 | 4.17 | 0.075 (0.006) | −0.478 | 0.039 | Inconclusive |
| B Elec. | Level | W1 | 4.21 | 0.027 (0.004) | −0.326 | 0.003 | Marginal |
| B Elec. | Log | W1 | 4.32 | 0.024 (0.003) | −0.333 | 0.002 | Marginal |
| B Elec. | Log + Temp | W1 | 3.73 | 0.036 (0.004) | −0.329 | 0.003 | Marginal |
| A Fuel | Level | W2 | 3.14 | 0.156 (0.008) | −0.803 | 0.055 | Inconclusive |
| A Fuel | Log | W2 | 3.15 | 0.166 (0.008) | −0.863 | 0.101 | Inconclusive |
| A Fuel | Log + Temp | W2 | 8.88 | 0.000 (0.000) | −1.103 | 0.000 | Cointegration |
| A Fuel | Log + Temp + SAR | W2 | 7.93 | 0.000 (—) | −0.461 | 0.620 | Cointegration (F) |
| B Elec. | Level | W2 | 4.79 | 0.019 (0.003) | −1.086 | 0.005 | Marginal |
| B Elec. | Log | W2 | 6.60 | 0.003 (0.001) | −0.991 | 0.001 | Marginal |
| B Elec. | Log + Temp | W2 | 6.71 | 0.001 (0.001) | −1.006 | 0.000 | Marginal |

Notes: $n = 199$ (W0)/180 (W1)/91 (W2); effective sample sizes 192/173/84 (77 for the SAR row); bootstrap 1999 replications; MC SE is the binomial Monte Carlo standard error of the boot $p$; "Marginal" indicates $p$ in the 0.04–0.07 seed-sensitive band, and electricity-margin verdicts are labelled Marginal throughout given the degenerate-case qualification in Section 4.2; the three $|\rho| > 1$ entries (W2) represent oscillatory convergence with implied AR roots satisfying $|\lambda| < 1$. The Log + Temp + SAR row is the seasonally corrected EV-era specification adopted in Section 3.4; its verdict rests on the joint $F$ statistic, and its ECT $t$ ratio is insignificant ($p = 0.620$, see Section 4.2).

Three $|\rho| > 1$ oscillatory convergence results in the EV-era window warrant explanation: with only 84 effective observations, long differenced terms and monthly dummies absorb substantial degrees of freedom, inflating the estimation variance of the error correction coefficient; with shorter fixed lags, $\rho$ returns to −0.81 (Model A) and −0.81 (Model B), with cointegration verdicts unchanged. CUSUM tests based on recursive residuals (Figure 2) show the full-sample headline specification remaining entirely within the 95% confidence band throughout. In the seasonally corrected EV-era specification, the fluctuation path exceeds the upper band over part of the intermediate sample before returning inside it near the sample end, while the formal CUSUM stability test does not reject parameter constancy ($p = 0.899$); the EV-era point estimates are accordingly treated with more caution than the full-sample results. Full diagnostic statistics for all specifications appear in Appendix A, Table A6.

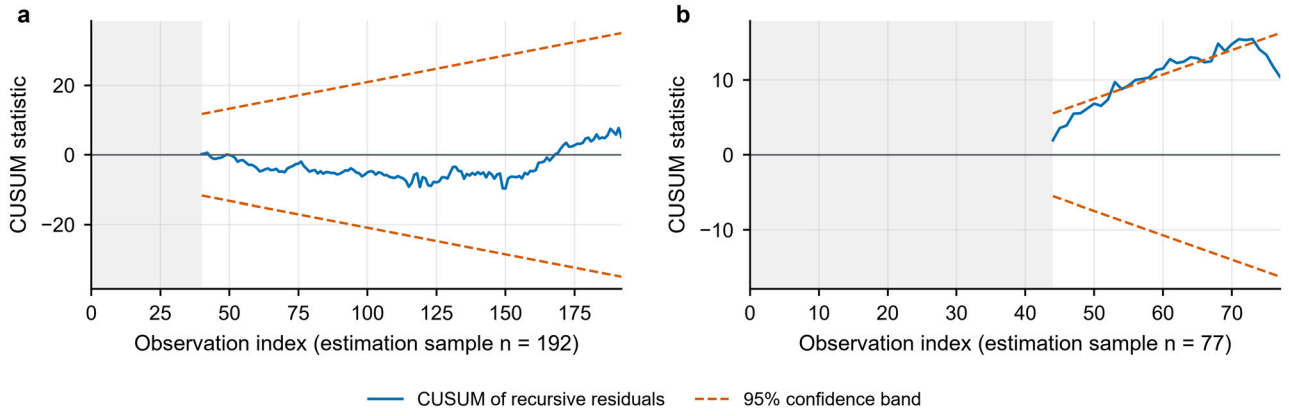


**Figure 2.** CUSUM tests of recursive residuals for parameter stability. (**a**) Full-sample specification ($n = 192$); (**b**) EV-era seasonally corrected specification ($n = 77$). Notes: The solid blue lines plot the cumulative sum of recursive residuals, and the dashed orange lines denote the 95% critical bounds. The full-sample statistics remain strictly within the critical bands; in the EV-era seasonally corrected specification the fluctuation path exceeds the upper band over part of the intermediate sample before returning inside it (Section 4.2), while the formal CUSUM test does not reject parameter constancy.

### *4.3. Long-Run Estimates: Fuel Substitution Margin*

Table 4 reports long-run coefficients for Model A. In the baseline full-sample specification (Column 1), the EV elasticity of −0.544 implies that a doubling of penetration (log increase of 0.69) is associated with a long-run gasoline consumption decrease of approximately 38%. Controlling for monthly mean temperature (Column 2) yields a virtually unchanged coefficient of −0.546, suggesting that weather variations do not confound this substitution relationship. The EV-era subsample (Columns 3 and 4) is where the seasonal correction of Section 3.4 binds: the uncorrected temperature-augmented estimate is −0.511 (0.042), while the seasonally corrected specification halves the point estimate to −0.266 (0.169, $p = 0.124$). We therefore read the EV-era evidence as directionally consistent but statistically fragile, and anchor the headline magnitude on the full-sample and handover windows, whose temperature-augmented specifications pass all residual diagnostics without correction (−0.546 and −0.616). The EV-era log form without temperature augmentation is diagnostic-clean (BG-LM(12) $p = 0.486$) and yields −0.490, but its bounds verdict is inconclusive (Table 3), so it corroborates the direction of the association rather than establishing EV-era cointegration.

Corresponding level-form estimations indicate that a one percentage point increase in EV penetration reduces gasoline consumption by 0.074% to 0.109% ($p < 0.001$). Crucially, across all 18 evaluated specifications (encompassing three estimation windows and six functional variants), the long-run coefficients of EV penetration remain uniformly negative, reinforcing the directional stability of the fuel substitution margin.

The estimated visitor elasticities reveal a clear pattern of asymmetric response across specifications. In the full sample, the positive partial sum elasticity of 0.093 indicates that a 10% increase in visitor arrivals is associated with a 0.93% long-run expansion in gasoline consumption. This modest response aligns with the lower bound of estimates reported in the broader tourism–energy literature (0.3–1.2) [15,16,37], reflecting Macau's transit- and gaming-oriented tourism model characterized by relatively low per-visitor transport fuel intensity. Conversely, the negative partial sum elasticity of 0.067 implies that an equivalent 10% contraction in arrivals reduces gasoline consumption by only 0.67%—approximately 72% of the expansionary impact. This persistent 28-percentage-point ratchet gap remains directionally stable across all evaluated models.

**Table 4.** Long-run coefficients, fuel margin (Model A).

| Variable | $A_R$ (W0) Log | $A_T$ (W0) Log + Temp | $A_T$ (W2) Log + Temp | $A_T$ (W2) Log + Temp + SAR |
|---|---|---|---|---|
| EV penetration (log) | −0.544 *** (0.060) | −0.546 *** (0.061) | −0.511 *** (0.042) | −0.266 (0.169) |
| Gasoline price POS | +0.226 ** (0.072) | +0.211 ** (0.076) | +0.054 (0.129) | −0.322 (0.448) |
| Gasoline price NEG | −0.047 (0.064) | −0.042 (0.066) | +0.014 (0.129) | +0.857 (0.652) |
| Visitor arrivals POS | +0.093 *** (0.014) | +0.091 *** (0.014) | +0.078 *** (0.013) | +0.179 * (0.069) |
| Visitor arrivals NEG | +0.067 *** (0.012) | +0.065 *** (0.012) | +0.045 *** (0.011) | +0.172 * (0.079) |
| Temperature | — | +0.011 (0.009) | −0.001 (0.009) | −0.002 (0.024) |
| Wald: price symmetry ($p$) | <0.001 | 0.002 | 0.842 | 0.055 |
| Wald: visitor symmetry ($p$) | 0.012 | 0.011 | <0.001 | 0.755 |

Notes: Parentheses contain delta-method standard errors. $p < 0.10$, * $p < 0.05$, ** $p < 0.01$, *** $p < 0.001$. Level-form EV coefficients (per percentage point): W0 −0.074 (0.014), W1 −0.109 (0.027), W2 −0.077 * (0.009). Wald tests are long-run symmetry restrictions $\theta^+ = \theta^-$. "—" indicates the variable is not included in that specification.

The elasticity magnitude requires upper-bound interpretation. Over the sample period, EV penetration (log form) rose 2.19 log points. Extrapolating from the full-sample elasticity of −0.544 implies a gasoline decline of approximately 70%; the level form, extrapolated over the in-sample 7.9 percentage point rise, implies a 50–60% decline; yet actual 2024 gasoline consumption was only about 20% below the 2019 level. The coefficient therefore absorbs not only electrification substitution but also structural factors trending with penetration over the same period, including post-pandemic cross-border travel contraction and internal combustion vehicle efficiency improvements. We interpret the −0.5 magnitude as an upper bound on the substitution effect, with the direction and the magnitude range (−0.27 to −0.62, see Section 4.6) as the primary conclusions.

Tourism variables behave in the direction of H3: the positive partial sum elasticity (0.078–0.093) exceeds the absolute value of the negative partial sum (0.045–0.067) in all three uncorrected headline specifications, with the long-run symmetry test rejected at 5% (full sample $p = 0.012$, uncorrected EV era $p < 0.001$); under the seasonal correction the EV-era visitor asymmetry is not retained (Wald $p = 0.755$, Table 4), consistent with the fragility documented in Section 4.6. Gasoline price partial sums show asymmetry in the full sample (Wald $p < 0.001$), the sign and magnitude of these coefficients exhibit sensitivity across estimation windows and lag specifications (Section 4.6), suggesting that price asymmetries should be interpreted with caution.

### *4.4. The Bounded Null on the Electricity Margin*

Table 5 reports the estimated long-run relationships for the electricity margin (Model B). Across eight of the nine evaluated specifications, EV penetration yields statistically insignificant coefficients. For instance, the full-sample log-form elasticity is −0.075 (SE = 0.105, $p = 0.475$), while the temperature-augmented log specification in the EV era yields −0.023 (SE = 0.048, $p = 0.637$), with level-form counterparts remaining similarly indistinguishable from zero across the full and W1 windows. The only exception emerges in the EV-era level-form model, which yields a marginally significant coefficient of −0.0147 (0.0066, $p = 0.029$). This estimate is form-dependent—log and temperature-augmented forms in the same window yield no detection—and its implied magnitude contradicts observed trends: extrapolating over the in-sample 7.7 percentage point penetration rise implies an import dependence decline of approximately 11 percentage points, while import dependence in the EV-era window has remained essentially flat. Consequently, this isolated result reflects functional-form sensitivity rather than a robust structural association.

**Table 5.** Long-run coefficients, electricity margin (Model B).

| Variable | B (W0) Level | $B_R$ (W0) Log | B (W2) Level | $B_T$ (W2) Log + Temp |
|---|---|---|---|---|
| EV penetration | −0.007 (0.018) | −0.075 (0.105) | −0.015 * (0.007) | −0.023 (0.048) |
| Diesel price POS | +0.274 (0.173) | +0.279 (0.171) | −0.355 * (0.135) | −0.267 (0.152) |
| Diesel price NEG | +0.235 (0.170) | +0.262 (0.174) | −0.250 (0.178) | −0.354 (0.180) |
| Visitor POS | −0.013 (0.018) | −0.006 (0.021) | +0.015 (0.013) | +0.013 (0.015) |
| Visitor NEG | −0.012 (0.015) | −0.012 (0.014) | +0.006 (0.013) | +0.009 (0.015) |
| Temperature | — | — | — | +0.029 * (0.012) |
| EV HAC(12) *p* | 0.697 | 0.475 | <0.001 | 0.329 |

Notes: Parentheses contain delta-method standard errors. $p < 0.10$, * $p < 0.05$. EV row forms differ by column—B (W0) and B (W2) are level-form coefficients (per percentage point); $B_R$ (W0) and $B_T$ (W2) are log-form elasticities. The four values are not directly comparable.

The evidence from Table 5 can be read at three levels. The first is point estimate consistency, where EV coefficients are uniformly negative across all four columns (−0.007 to −0.075), consistent with the substitution logic of the fuel margin—if EVs do not displace fuel, the electricity margin should show no systematic association. The second is statistical significance, where the eight insignificant specifications constitute the principal "no detectable effect" evidence, while the sole significant exception is downgraded on the basis of form dependence and implied-magnitude contradiction. The third is power, where the full-sample log-form minimum detectable effect of 0.209 corresponds to an import dependence change of 21 percentage points (translated by the in-sample penetration rise), while the observed span of the series is only 38 percentage points—meaning the full-sample and handover "insignificance" provides limited statistical constraint. Only the EV-era window (MDE 0.100, approximately 13 percentage points) has effective constraining power. Synthesizing these three levels indicates that EV penetration at its current scale does not constitute a detectable disturbance to electricity import structure, and even if an effect exists, its magnitude is bounded by the EV-era confidence interval upper limit (import dependence change not exceeding 13 percentage points).

The evidentiary weight of the null depends on statistical power. When approximating the minimum detectable effect by twice the standard error, the full-sample and handover log forms yield 0.209 and 0.379—the latter exceeds the 0.382 observed span of the import dependence series, indicating that the "insignificance" in these two windows is of limited empirical constraint. The EV-era log-form MDE is 0.100, with 95% CI [−0.134, +0.066], implying an import dependence change interval of [−0.27, +0.13] over the in-sample penetration rise, which confirms that if a true effect exists, its magnitude is insufficient to drive import dependence beyond the sample's fluctuation range. This is confirmed by an order-of-magnitude calculation: as of July 2026, the EV fleet numbers approximately 20,000 vehicles. Disaggregating by fleet composition—EV cars (approximately 12,000) at 1200–1500 kWh/year and electric motorcycles (approximately 8000) at 600–800 kWh/year—annual charging of approximately 19–25 GWh represents 0.30–0.39% of 2025 total electricity consumption (approximately 6310 GWh). The bounded null and the order-of-magnitude calculation mutually corroborate, establishing H2 in the sense of "no detectable association + bounded + power accounting." This framing carries an epistemic distinction worth making explicit: the evidence constitutes an absence of detectable association at attainable power, combined with bounds on any underlying effect; it does not demonstrate an effect of exactly zero, and it is the bounds, not the insignificance, that carry the inferential weight.

As a companion test for the electricity margin, we repeated the Model B specification with ln(total electricity consumption) as the dependent variable. In this test, the EV penetration long-run coefficient is insignificant in both the full sample ($p = 0.164$) and the EV era

($p = 0.587$), corroborating the import dependence results that EV penetration has altered neither the quantity nor the structure of electricity.

Diesel price coefficients flip signs across windows (positive and insignificant in the full sample, negative in the EV era), consistent with the non-robustness of price asymmetry in Section 4.3, and are therefore not interpreted as stable structural effects. The temperature coefficient is significantly positive in the EV era (0.029, $p = 0.021$)—a 1 °C increase is associated with approximately 3 percentage points higher import dependence, consistent with high-temperature load being predominantly import-served. This coefficient is insignificant in the full sample and sensitive to lag selection (appendix); it is treated as suggestive sub-sample evidence.

### *4.5. Dynamic Multipliers and Asymmetric Paths*

Figure 3 presents the cumulative dynamic multiplier paths for ±10% permanent shocks to gasoline prices and visitor arrivals under the full-sample temperature-augmented specification, the window in which the asymmetry evidence is diagnostically clean and robust to seasonal augmentation. Visitor shock responses converge smoothly to their long-run levels within 8–12 months; the response to a +10% expansion converges to approximately +0.87%, whereas the response to a −10% contraction converges to approximately −0.62%, so the expansion elasticity (0.092) exceeds the contraction elasticity (0.065) and the paths visually depict the ratcheted asymmetry. Price shock responses display transitory oscillations over the initial months before stabilizing, with only the positive price response significantly different from zero in the long run (+2.0% versus +0.4%, the latter insignificant). Across both dimensions, the dynamic multipliers remain strictly bounded and non-explosive, corroborating the stable adjustment speeds implied by the error correction estimates.

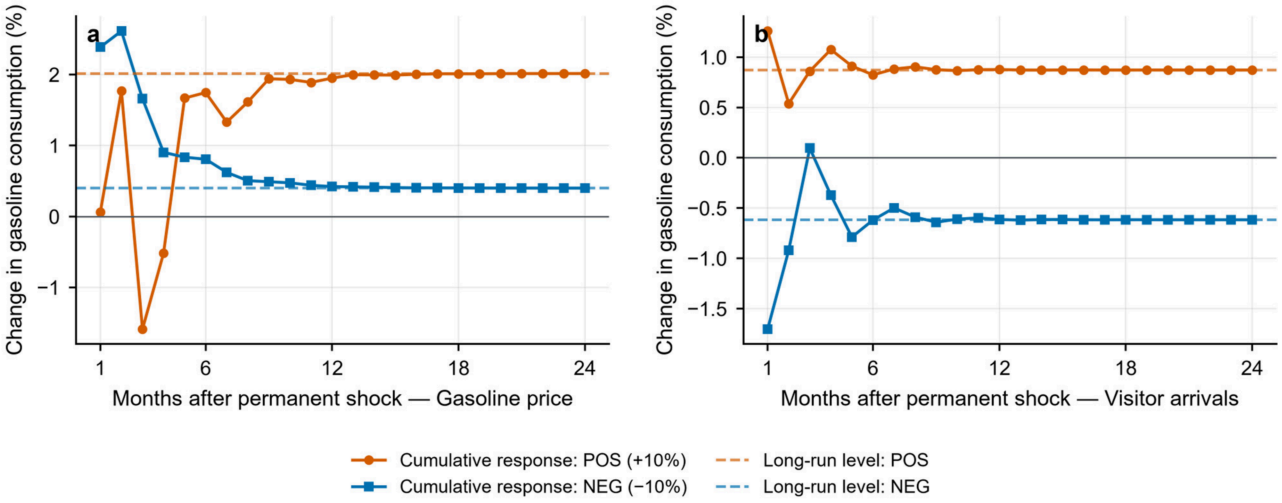


**Figure 3.** Cumulative dynamic multiplier paths of gasoline consumption under asymmetric shocks, full-sample temperature-augmented specification ($n = 192$). (**a**) Response to ±10% permanent shocks in gasoline retail prices; (**b**) Response to ±10% permanent shocks in visitor arrivals.

### *4.6. Robustness*

Table 6 summarizes all empirical perturbations. Regarding lag selection protocols, point estimates remain stable across alternative specifications. Specifically, under the AIC@4/4 protocol, the full-sample log-form EV coefficient is −0.442 ($p < 0.001$), closely matching the baseline magnitude of −0.544. Conversely, lag expansion primarily affects statistical test performance rather than elasticity estimates, as relaxing the search grid raises the bounds test $p$-value to 0.178 and the visitor asymmetry Wald $p$-value to 0.619. Fixed

baseline lags serve as a bootstrap seed stability check, where identical model structures confirm that bootstrap $p$-value differences reflect only Monte Carlo noise while point estimates remain unchanged. This pattern confirms that expanding parameters from 35 to 42 in finite samples reduces test power due to parameter proliferation rather than signaling the absence of structural relationships.

**Table 6.** Robustness summary.

| Perturbation | Specification | EV $\beta$ | EV $p$ | Visitor Wald $p$ | Verdict |
|---|---|---|---|---|---|
| Baseline | $A_R$ (W0) | −0.544 | <0.001 | 0.012 | — |
| Lag AIC@4/4 | $A_R$ (W0) | −0.442 | <0.001 | 0.619 | $\beta$ stable; tests weakened |
| Pandemic short | $A_T$ (W2) | −0.603 | <0.001 | 0.728 | EV stable; W2 ratchet pandemic-driven |
| Pandemic long | $A_T$ (W2) | −0.559 | <0.001 | 0.019 | Ratchet survives long dummy |
| Charging points | $A_T$ (W2m) fixed | −0.518 | <0.001 | 0.111 | EV stable |
| Gaming replaces visitors | $A_R$ (W0) | −0.530 | <0.001 | <0.001 | H1, H3 strengthened |
| EV = asinh | A (W0) | −0.472 | <0.001 | 0.005 | Stable |
| EV = $\log_{10}$ | A (W0) | +0.006 | 0.993 | 0.339 | Form fails; disclosed |
| EV linear detrended | $A_T$ (W0) | −0.089 | <0.001 | 0.247 | Shrunk 84%; trend carries ID |
| EV quadratic detrended | $A_T$ (W0) | −0.052 | 0.525 | — | Not significant |
| Seasonal SAR | $A_T$ (W2) | −0.266 | 0.124 | 0.755 | Adopted for $A_T$ (W2); W2 log range −0.27 to −0.51 |
| HAC(12) | B (W2) | −0.015 | <0.001 | — | B inference robust |
| ICE renewal control | $A_T$ (W0) | −0.496 | <0.001 | 0.0003 | EV stable; renewal +0.24 (fleet growth) |
| Car-only EV share | $A_T$ (W0) | −0.581 | <0.001 | 0.015 | EV stable; borderline BG12 0.049 in AT |

The robustness checks yield three central insights. First, the direction of H1 is highly robust, whereas its EV-era precision is not. With the exception of the common logarithm transformation, EV coefficients remain uniformly negative across all perturbations, spanning the range of −0.27 to −0.62; the seasonal correction required by the EV-era diagnostics (Table A3) halves that window's point estimate to −0.27 and removes its conventional significance, so the range is read as a span of point estimates rather than a band of homogeneous precision. The divergence in the common logarithm (log10) specification stems from two technical reasons: the transformation requires ev > 0, thereby excluding the 2010–2018 zero-penetration period, and it models log10(ev) rather than log10(1 + $ev$), limiting comparability with the baseline. A fleet-renewal control (cumulative post-2010 ICE registrations as a share of the fleet, in logs) addresses the ICEV-efficiency confound directly: it absorbs roughly nine percent of the full-sample EV coefficient (−0.546 to −0.496 in the temperature-augmented specification; −0.544 to −0.494 in the plain log form) while entering positively itself (+0.24, $p = 0.002$), a sign pattern indicating that the proxy captures fleet expansion rather than efficiency gains per vehicle; the EV association survives with tighter standard errors and clean diagnostics (Table 6). A car-only penetration check addresses the numerator-composition question directly: restricting EV penetration to electric passenger cars yields −0.577 and −0.581 in the two full-sample specifications (both

$p < 0.001$, Table 6), with the temperature-augmented variant showing borderline residual seasonality (BG-LM(12) $p = 0.049$); the association is therefore not driven by the motorcycle component. Second, parameter identification is fundamentally anchored in the diffusion trend. Linear detrending attenuates the coefficient to approximately one-sixth of the baseline, while quadratic detrending renders it statistically insignificant, confirming that H1 fundamentally captures a long-run equilibrium co-movement driven by structural adoption trends (full perturbation estimates in Appendix A, Table A5). Third, evidence for H3 is primarily anchored in the full sample and handover window (Wald $p \leq 0.016$ in both, and stable under seasonal augmentation), whereas the EV-era ratchet is fragile: it survives the extended pandemic dummy but disappears under the diagnostic-required seasonal correction (Wald $p = 0.755$). Importantly, the statistical significance of tourism asymmetry exhibits functional-form sensitivity, emerging reliably under the logarithmic EV specification while attenuating under the level form (W0 $p = 0.130$, W1 $p = 0.831$, W2 $p = 0.113$). Under the log-form specification, the asymmetry remains robust to pandemic controls (full-sample short-form $p = 0.046$, long-form $p = 0.006$; handover window $p = 0.018/0.026$) and to the January 2023 "Macau Vehicle Northbound" policy break (full-sample $p = 0.034$), establishing that the asymmetric visitor response is robust across policy shocks conditional on the logarithmic formulation.

## 5. Discussion and Policy Implications

### *5.1. The Bounded Null and Boundary Conditions for the EV–Grid Literature*

Rather than contradicting existing EV-grid scholarship, our null finding calibrates critical boundary conditions for this literature. Charging load modeling and distribution network impact studies [1,2,4,6] predominantly analyze distribution systems characterized by high penetration and unmanaged charging, where the proposition that grid stress escalates alongside adoption rests on solid ground. Macau occupies the opposite end of that applicability spectrum, defined by charging loads below 0.4% of total consumption, saturated supply reliability, and load growth readily absorbed by import contracts and local peak-shaving units. At this end, a null effect on the electricity margin represents an empirical inevitability dictated by physical scale. When new load sits two orders of magnitude below the system's inherent monthly volatility, no aggregate-level time-series method should—or can—detect an effect.

A numerical comparison with the broader EV–grid literature is instructive. Suski et al. [1] showed in their Maldives simulation that at 20% EV penetration, charging load constitutes approximately 15% of system peak, generating significant distribution stress. In contrast, Macau's current penetration of approximately 8% generates charging load below 0.4%—a two-order-of-magnitude gap that clarifies why aggregate empirical records show none of the operational strain anticipated by engineering simulations. Nogueira et al. [2] assumed 30% penetration for Portugal by 2030, and Gay et al. [11] emphasized capacity constraints in small island systems, both presupposing penetration levels far above current reality. This comparison clearly demarcates methodological boundaries, where engineering simulations are tailored to high-penetration, distribution-level forward planning, whereas empirical cointegration evaluations address system-level conditions during early-to-intermediate adoption stages. As fleet scale grows, these two analytical paths will naturally converge, rendering the bounded benchmarks and power constraints established in this paper a reliable baseline to evaluate future grid impacts.

The behavior of charging infrastructure is a background variable not fully identified but worth recording. The 2022 pulse expansion of charging points is temporally coupled with the acceleration of EV penetration, and the EV coefficient remains stable when charging points enter the equation in robustness checks—consistent with "infrastructure as a facilitation

variable rather than a stressor" [11]. In a reliability-saturated system, charging network expansion primarily alters adoption behavior, not load structure.

### *5.2. Fuel Margin Elasticity and Magnitude Benchmarks*

The long-run fuel margin elasticity (log-family point estimates from −0.27 under the EV-era seasonal correction to −0.62 in the handover window) falls on the extension of two strands of existing evidence. Measurement and life-cycle studies [8,9,31,43] provide per-vehicle energy substitution ratios implying fleet-level elasticities significantly below unity; our estimates align directionally with these micro-benchmarks while serving as an empirical upper bound. In magnitude terms, our elasticity of −0.5 is broadly consistent with the literature's implied substitution expectations. Specifically, Wang et al.'s [8] real-world data (EV per-kilometer energy consumption at 30–40% of conventional vehicles) imply a 60–70% fuel saving per vehicle replaced under one-for-one substitution (a vehicle-level ratio rather than an elasticity). Translating our elasticity of −0.5 across the in-sample log penetration rise (2.19) yields an implied decline of 50–60%, situated at the lower end of that range, where the gap partly reflects the net substitution remaining after common-trend factors are absorbed. Compared with Shi et al.'s [31] Beijing taxi case, which documented fuel consumption declines exceeding one-for-one expectations due to compounding mileage reductions, our gasoline margin encompasses private vehicles (approximately 50% of the fleet), explaining why a moderate fleet-wide elasticity emerges naturally from vehicle composition.

This upper-bound framing carries direct implications for policy calculations. Using this elasticity to forecast fuel demand and import contraction yields a conservative lower bound, suggesting that actual volume declines will materialize more gradually. Conversely, any "electrification dividend" calculation based on this elasticity will overstate gains.

### *5.3. Tourism Ratchet and Convergence with Asymmetric Evidence*

The ratcheted asymmetry of the tourism–gasoline relationship aligns directionally with a robust pattern in the tourism–energy–environment literature, where expansion-side long-run coefficients consistently exceed contraction-side absolute values [15,16,36,37]. An explanation consistent with our results is the stickiness of tourism transport service capacity. Gasoline-relevant service capacity—taxi and ride-hailing licenses—expands during tourism peaks and subsequently faces maintenance costs and regulatory contract-term constraints, whereas cross-border coaches and hotel shuttles operate primarily on diesel and thus affect the diesel margin rather than the gasoline margin examined here. Because de-capacitization during demand contractions proceeds more slowly than capacity deployment during expansions, contraction-side fuel savings fall short of expansion-side fuel increments. Macau's two closest studies [13,14] confirmed tourism–energy linkages via wavelet coherence and structural VAR, respectively, and our findings advance this strand of scholarship by demonstrating that this linkage is inherently asymmetric on the transport fuel margin. For tourism cities, this implies that fuel demand planning cannot extrapolate under symmetric assumptions, as fuel rebound during tourism revivals will be faster than the decline during equivalent contractions. The asymmetric reading is conditional: the pattern attenuates under the level form and, in the EV era, under seasonal correction (Section 4.6), so the planning implication attaches most strongly to the long full-sample horizon.

### *5.4. Policy Implications*

The empirical findings translate into three targeted policy implications grounded in the observed structural boundaries.

First, regarding the positioning of charging infrastructure, in an import-dominated and reliability-saturated system such as Macau's, the charging network currently functions as a facilitation variable for electrification adoption rather than a source of grid stress. Infrastructure planning can therefore adopt a "follow demand, lead modestly" strategy without imposing artificial supply restrictions on grid-security grounds.

Second, energy balance accounting, import logistics, and fuel expenditure planning must adapt to structural fuel substitution. To illustrate the magnitude, extrapolating from the upper-bound elasticity ($-0.5$), an increase in Macau's EV penetration from the current level of approximately 8% to approximately 16% (a log increase of 0.70) implies an additional gasoline decline of approximately 35% ($0.70 \times 0.5$); calibrating this projection to the actual decline (a "true" elasticity of approximately $-0.25$) yields a contraction of approximately 18%. Under either calibration, gasoline imports are set to contract cumulatively by more than thirty percent from their historical peak within three to five years. One fiscal implication deserves precision in the Macau context: unlike many jurisdictions, Macau levies no fuel excise, as petroleum products were removed from the consumption tax schedule in 2008 (Law No. 8/2008, Macao Official Gazette, 1st Series, No. 34), so the contraction bears on import volumes, storage and logistics contracts, and household and business transport fuel expenditure rather than on fuel tax receipts. The planning burden is therefore physical and contractual: fuel import scheduling and terminal storage commitments should be revisited against a permanently lower demand trajectory, and any future road-user charging or carbon-pricing design would face a shrinking fuel base on the conventional-vehicle side alongside a growing electricity base on the EV side, a compositional shift that favors instruments priced per vehicle-kilometre rather than per litre. This shift represents a permanent trend inflection rather than a cyclical fluctuation.

Third, for tourism cycle management, transport fuel demand responds asymmetrically to visitor fluctuations. Energy and transport authorities should anticipate a faster-than-linear fuel recovery during tourism revivals and schedule fuel imports and cross-border capacity accordingly.

### *5.5. Limitations*

Five primary limitations define the scope of the conclusions. First, parameter identification inherently relies on the diffusion trend of EV penetration. Linear detrending attenuates the coefficient by approximately 84%, while quadratic detrending renders it statistically insignificant. Because common-trend dynamics cannot be empirically decoupled from pure technological substitution within aggregate time series, the upper-bound specification accurately captures the structural boundary of this association. Second, the empirical setting centers on a single economy. Macau's high import dependence, tourism intensity, and saturated grid reliability represent a specialized institutional context, meaning direct extrapolation of specific elasticity estimates to larger or differently structured systems warrants prudent consideration. Nonetheless, the dual-margin analytical framework remains broadly portable. Third, data disaggregation constraints bind at several levels and are the principal obstacle to sharper attribution. Gasoline consumption is published only as a single aggregate, so it cannot be decomposed by vehicle class, and the distinct diffusion dynamics of passenger cars (additive adoption layered on a growing fleet) and motorcycles (direct displacement within a shrinking fleet) are captured only through fleet-level aggregates. The fleet-renewal control of Section 4.6 illustrates the resulting identification ceiling: cumulative ICE registrations proxy fleet expansion and per-vehicle efficiency improvement simultaneously, enter with a positive sign that reflects the former, and thus prevent a clean read of the latter. No monthly series distinguishes fuel use by vehicle age, engine class, or usage intensity (taxis versus private cars), and charging infrastructure data are available as public

point counts rather than delivered energy, so load-side attribution likewise remains physical and indirect. Fourth, because electricity purchase prices are proprietary contract information, the cost-transmission channel of imported power remains unobservable, restricting the empirical evaluation of the electricity margin to physical quantities and dispatch shares. Fifth, weak exogeneity of the regressors remains an assumption: the Granger precedence evidence of Section 3.3 supports the visitor-to-fuel direction but does not constitute full identification, and no external instrument is available at monthly frequency.

## 6. Conclusions

Focusing on Macau from January 2010 through July 2026, this paper employs a nonlinear autoregressive distributed lag framework to evaluate the energy effects of transport electrification simultaneously across two margins. On the fuel margin, the long-run negative equilibrium association between EV penetration and gasoline consumption is directionally uniform across all 18 baseline specifications and 15 perturbation categories, with log-form point estimates spanning −0.27 to −0.62; its statistical firmness is concentrated in the full and handover windows, while the EV-era estimate is halved to −0.27 and loses conventional significance under the diagnostic-required seasonal correction. Because identification captures structural trend co-movements, this elasticity operates as an empirical upper bound on fuel displacement. The association is identified from co-movement with the diffusion trend: the fleet-renewal check bounds the ICEV-efficiency confound at roughly one-tenth of the coefficient, and the residual attribution between electrification and co-trending structural change cannot be split further with aggregate data. On the electricity margin, no detectable long-run association exists between EV penetration and electricity import dependence, as eight of nine specifications yield insignificant coefficients and the solitary significant estimate reflects functional-form sensitivity. Power accounting confirms that the EV-era confidence interval upper bound restricts any plausible change in import dependence to within the sample's fluctuation range, a finding directly corroborated by physical load calculations indicating that aggregate charging demands constitute less than 0.4% of total consumption. A companion test using total electricity consumption as the dependent variable corroborates this neutrality. Regarding dynamic asymmetry, tourism inflows exert an asymmetric long-run effect on gasoline consumption consistent with a ratchet, where the elasticity with respect to visitor expansions (0.078–0.093) exceeds that of contractions (0.045–0.067). This asymmetry is anchored in the full and handover samples, surviving pandemic and cross-border travel policy breaks under the log form, while attenuating under the level form and under the EV-era seasonal correction.

These empirical insights synthesize into a coherent policy perspective. In a constraints-driven tourism economy characterized by import dominance and saturated reliability, electrification is structurally reshaping the fuel ledger while the electricity ledger remains undisturbed. Consequently, charging infrastructure currently functions as an adoption facilitator rather than a grid stressor, while fuel import planning and storage contracting should reserve adequate space for a structural contraction that proceeds faster than linear projections suggest; in Macau's specific fiscal setting, where no fuel excise applies, the adjustment burden falls on physical supply chains and fuel expenditure rather than on tax receipts.

Future research can advance along three promising directions. First, multi-country or regional panel studies could test the external validity of the dual-margin framework. Second, continuous re-evaluations of the electricity margin null will become valuable as fleet scale and charging load shares expand. Finally, integrating high-frequency, pile-level micro data would enable direct evaluations of localized distribution-level load effects

presupposed by engineering literature, constructively complementing the system-level neutrality documented in this study.

**Author Contributions:** Conceptualization, C.W.; methodology, Y.Y. (Yifen Yin); validation, Y.Y. (Yuanyuan Yu); formal analysis, W.I.H.; data curation, W.I.H.; writing—original draft preparation, W.I.H.; writing—review and editing, Y.Y. (Yifen Yin), Y.Y. (Yuanyuan Yu) and C.W.; visualization, W.I.H.; supervision, Y.Y. (Yifen Yin); project administration, C.W. All authors have read and agreed to the published version of the manuscript.

**Funding:** This research is supported by Macao Polytechnic University, RP/FCHS-02/2026.

**Data Availability Statement:** The original data presented in the study are openly available in FigShare at https://doi.org/10.6084/m9.figshare.34333317.

**Acknowledgments:** Generative AI tools were used for language translation (Chinese to English) and text polishing. All research design, data analysis, interpretation of results, and substantive content are the authors' own work.

**Conflicts of Interest:** The authors declare no conflicts of interest.

## Abbreviations

The following abbreviations are used in this manuscript:

| | |
|---|---|
| NARDL | Nonlinear autoregressive distributed lag |
| EV | Electric vehicle |
| V2G | Vehicle-to-grid |
| DSEC | Macau Statistics and Census Service |
| DICJ | Gaming Inspection and Coordination Bureau |
| SMG | Macao Meteorological and Geophysical Bureau |
| AIC | Akaike Information Criterion |
| HAC | Heteroskedasticity and autocorrelation consistent |

## Appendix A

**Table A1.** Unit Root Tests, Handover Window (W1: January 2010–December 2024).

| Series | ADF $p$ (Level) | ADF $p$ ($\Delta$) | ADF Verdict | KPSS $\eta$ (Level) | KPSS Verdict (5%) | ADF $p$ (Level, Trend) | KPSS$_\tau$ $p$ (Level, Trend) |
|---|---|---|---|---|---|---|---|
| ln g | 0.213 | 0.000 | $I(1)$ | — | — | 0.831 | — |
| imp | 0.000 | 0.000 | $I(0)$ | — | — | 0.000 | — |
| ev | 0.992 | 1.000 | $I(2)$ | — | — | 1.000 | $\leq$0.01 |
| ln(1 + ev) | 0.878 | 0.937 | $I(2)$ | — | — | 0.938 | $\leq$0.01 |
| ln $p_g$ | 0.516 | 0.000 | $I(1)$ | — | — | 0.649 | — |
| ln $p_d$ | 0.215 | 0.000 | $I(1)$ | — | — | 0.328 | — |
| ln v | 0.010 | 0.000 | $I(0)$ | — | — | 0.033 | — |
| temp | 0.282 | 0.000 | $I(1)$ | — | — | 0.069 | — |

Notes: ADF includes intercept, lag selection by AIC (max 12). KPSS cross-validation was conducted for W0 and W2 only; the conclusions carry over. "—" = not tested. Referenced in Table 2 notes. The trend columns follow Table 2; both EV forms reject trend-stationarity (KPSS$_\tau$ $p \leq 0.01$) while the trend-augmented ADF does not reject the unit root ($p = 1.000$ and 0.938).

**Table A2.** Lag-Rule Sensitivity Comparison.

| Model | Window | Lag Rule | $(p, q)$ | $F$ | Boot $p$ | EV $\beta$ | EV $p$ | Visitor Wald $p$ |
|---|---|---|---|---|---|---|---|---|
| Fuel ($A_R$) | W0 | AIC@3/3 (baseline) | (2, 3) | 5.15 | 0.044 | −0.544 | 0.0000 | 0.012 |
| Fuel ($A_R$) | W0 | AIC@4/4 | (4, 4) | 4.24 | 0.177 | −0.442 | 0.0001 | 0.619 |
| Fuel ($A_R$) | W0 | Fixed baseline | (2, 3) | 5.15 | 0.043 | −0.544 | 0.0000 | 0.012 |
| Fuel ($A_T$) | W2 | AIC@3/3 (baseline) | (1, 2) | 8.88 | 0.000 | −0.511 | 0.0000 | 0.000 |
| Fuel ($A_T$) | W2 | AIC@4/4 | (4, 4) | 2.41 | 0.291 | −0.419 | 0.0063 | 0.568 |
| Fuel ($A_T$) | W2 | Fixed baseline | (1, 2) | 8.88 | 0.000 | −0.511 | 0.0000 | 0.000 |
| Electricity ($B_R$) | W0 | AIC@3/3 (baseline) | (1, 0) | 4.78 | 0.017 | −0.075 | 0.4747 | 0.677 |
| Electricity ($B_R$) | W0 | AIC@4/4 | (1, 0) | 4.81 | 0.010 | −0.070 | 0.5053 | 0.670 |
| Electricity ($B_R$) | W0 | Fixed baseline | (1, 0) | 4.78 | 0.013 | −0.075 | 0.4747 | 0.677 |
| Electricity ($B_T$) | W2 | AIC@3/3 (baseline) | (1, 3) | 6.71 | 0.001 | −0.023 | 0.6373 | 0.647 |
| Electricity ($B_T$) | W2 | AIC@4/4 | (1, 4) | 5.79 | 0.010 | −0.055 | 0.3063 | 0.198 |
| Electricity ($B_T$) | W2 | Fixed baseline | (1, 3) | 6.71 | 0.000 | −0.023 | 0.6373 | 0.647 |

Notes: Three lag-selection protocols are reported side by side (Section 3.4). "Fixed baseline" retains the $(p, q)$ selected under AIC@3/3; since this is the same model by construction, differences in boot $p$ reflect only Monte Carlo noise. Referenced in Section 4.6.

**Table A3.** Seasonal Autoregressive Augmentation Sensitivity.

| Specification | Treatment | $(p, q)$ | BG-LM(12) $p$ | $F$ | Boot $p$ | $\rho$ | EV $\beta$ | EV $p$ | Visitor Wald $p$ |
|---|---|---|---|---|---|---|---|---|---|
| B W2 | Baseline | (2, 3) | 0.000 | — | — | −1.086 | −0.015 | 0.0294 | 0.189 |
| B W2 | SAR ($\Delta y_{t-12}$) | (1, 3) | 0.003 | 6.66 | 0.000 | −0.794 | −0.023 | 0.0205 | 0.048 |
| $B_R$ W2 | Baseline | (1, 3) | 0.000 | — | — | −0.991 | −0.036 | 0.4753 | 0.239 |
| $B_R$ W2 | SAR ($\Delta y_{t-12}$) | (1, 3) | 0.001 | 7.46 | 0.001 | −0.833 | −0.114 | 0.0811 | 0.019 |
| $B_T$ W2 | Baseline | (1, 3) | 0.004 | — | — | −1.006 | −0.023 | 0.6373 | 0.647 |
| $B_T$ W2 | SAR($\Delta y_{t-12}$) | (2, 3) | 0.016 | 6.72 | 0.000 | −1.076 | −0.113 | 0.0213 | 0.026 |
| $A_T$ W2 | Baseline | (1, 2) | 0.012 | — | — | −1.103 | −0.511 | 0.0000 | 0.000 |
| $A_T$ W2 | SAR ($\Delta y_{t-12}$) | (1, 3) | 0.244 | 7.93 | 0.000 | −0.461 | −0.266 | 0.1240 | 0.755 |
| $A_R$ W2 | Baseline | (2, 3) | 0.486 | — | — | −0.863 | −0.490 | 0.0000 | 0.003 |
| $A_R$ W2 | SAR ($\Delta y_{t-12}$) | (1, 3) | 0.143 | 10.37 | 0.000 | −0.524 | −0.313 | 0.0203 | 0.482 |
| $A_T$ W0 | Baseline | (2, 3) | 0.261 | — | — | −0.493 | −0.546 | 0.0000 | 0.011 |
| $A_T$ W0 | SAR ($\Delta y_{t-12}$) | (2, 3) | 0.115 | 4.08 | 0.071 | −0.494 | −0.536 | 0.0000 | 0.016 |

Notes: SAR = seasonal autoregressive augmentation (adding $\Delta y_{t-12}$ to the ECM). SAR does not eliminate seasonal serial correlation in the B-class W2 specifications (BG-LM(12) $p$ remains $< 0.05$), for which HAC(12) inference is used instead (Table A4); where the correction does remove the residual seasonality (the A-class W2 equations), it is adopted as the primary treatment (Section 3.4). Referenced in Section 3.4.

**Table A4.** HAC(12) Inference for the Electricity Margin.

| Specification | EV $\beta$ | SE (HAC 12) | $p$ (OLS) | $p$ (HAC 12) |
|---|---|---|---|---|
| B (W2) level | −0.0147 | 0.0030 | 0.0294 | 0.0000 |
| $B_R$ (W2) log | −0.0359 | 0.0203 | 0.4753 | 0.0825 |
| $B_T$ (W2) log + temp | −0.0226 | 0.0229 | 0.6373 | 0.3288 |
| $A_T$ (W2) log + temp | −0.5113 | 0.0262 | 0.0000 | 0.0000 |

Notes: Newey–West HAC standard errors with 12 lags. The fuel margin specification ($A_T$ W2) is included for comparison. The sole significant electricity margin estimate (B W2 level) survives HAC but disappears under the AIC@4/4 lag rule (Table A2), confirming its form- and rule-dependence. Referenced in Section 4.4 and Table 5.

**Table A5.** Additional Robustness Variants.

| Specification | $(p, q)$ | EV $\beta$ | EV $p$ | Visitor Wald $p$ |
|---|---|---|---|---|
| A (log) W0 + pandemic short | (2, 3) | −0.544 | 0.0000 | 0.046 |
| A (log) W0 + pandemic long | (2, 3) | −0.577 | 0.0000 | 0.006 |
| A (level) W0 + pandemic short | (2, 3) | −0.082 | 0.0000 | 0.173 |
| A (level) W0 + pandemic long | (2, 3) | −0.056 | 0.0008 | 0.266 |
| A (log) W1 + pandemic short | (2, 3) | −0.684 | 0.0000 | 0.018 |
| A (log) W1 + pandemic long | (2, 3) | −0.583 | 0.0000 | 0.026 |
| A (level) W1 + pandemic short | (2, 3) | −0.140 | 0.0004 | 0.491 |
| A (level) W1 + pandemic long | (2, 3) | −0.069 | 0.0415 | 0.706 |
| A (level) W0 baseline | (2, 3) | −0.074 | 0.0000 | 0.130 |
| A (level) W1 baseline | (2, 3) | −0.109 | 0.0001 | 0.831 |
| A W0 + Macau Northbound | (2, 3) | −0.556 | 0.0000 | 0.034 |
| A (level) W0 + Macau Northbound | (2, 3) | −0.063 | 0.0004 | 0.443 |
| A W2 + Macau Northbound | (2, 3) | −0.483 | 0.0000 | 0.026 |
| A (level) W2 + Macau Northbound | (3, 3) | −0.072 | 0.0000 | 0.119 |
| EV → total electricity (W0) | (3, 2) | −0.193 | 0.1639 | 0.209 |
| EV → total electricity (W2) | (3, 2) | 0.029 | 0.5873 | 0.030 |

Notes: Pandemic dummies: short = Feb–Jun 2020; long = Feb 2020–Dec 2022. Macau Northbound = step dummy from Jan 2023. EV → total electricity uses ln(total electricity consumption) as the dependent variable. Level form = EV penetration enters in percentage points; log form = ln(1 + ev). Referenced in Sections 4.6 and 6.

**Table A6.** Full Diagnostic Statistics.

| Model | BG-LM(1) $p$ | BG-LM(12) $p$ | JB $p$ | ARCH(1) $p$ | CUSUM $p$ | CUSUM Cross | $R^2$ | adj $R^2$ |
|---|---|---|---|---|---|---|---|---|
| A W0 level | 0.065 | 0.388 | 0.000 | 0.770 | 0.966 | No | 0.918 | — |
| $A_R$ W0 log | 0.073 | 0.456 | 0.000 | 0.818 | 0.860 | No | 0.923 | — |
| $A_T$ W0 log + temp | 0.068 | 0.261 | 0.000 | 0.865 | 0.828 | No | 0.925 | — |
| A W1 level | 0.173 | 0.298 | 0.000 | 0.762 | 0.974 | No | 0.930 | — |
| $A_R$ W1 log | 0.426 | 0.524 | 0.000 | 0.438 | 0.894 | No | 0.931 | — |
| $A_T$ W1 log + temp | 0.427 | 0.294 | 0.000 | 0.461 | 0.853 | No | 0.932 | — |
| A W2 level | 0.073 | 0.427 | 0.042 | 0.457 | 0.810 | No | 0.953 | — |
| $A_R$ W2 log | 0.255 | 0.486 | 0.005 | 0.392 | 0.749 | No | 0.954 | — |
| $A_T$ W2 log + temp | 0.034 | 0.012 | 0.006 | 0.211 | 0.725 | No | 0.949 | — |
| B W0 level | 0.498 | 0.406 | 0.000 | 0.011 | 0.899 | No | 0.240 | — |
| $B_R$ W0 log | 0.426 | 0.486 | 0.000 | 0.010 | 0.898 | No | 0.241 | — |
| $B_T$ W0 log + temp | 0.417 | 0.469 | 0.000 | 0.011 | 0.898 | No | 0.241 | — |
| B W1 level | 0.503 | 0.515 | 0.000 | 0.025 | 0.908 | No | 0.240 | — |
| $B_R$ W1 log | 0.431 | 0.557 | 0.000 | 0.022 | 0.891 | No | 0.242 | — |
| $B_T$ W1 log + temp | 0.466 | 0.507 | 0.000 | 0.026 | 0.894 | No | 0.244 | — |
| B W2 level | 0.139 | 0.000 | 0.114 | 0.089 | 0.953 | No | 0.648 | — |
| $B_R$ W2 log | 0.354 | 0.000 | 0.187 | 0.184 | 0.974 | Yes | 0.652 | — |
| $B_T$ W2 log + temp | 0.910 | 0.004 | 0.740 | 0.045 | 0.990 | No | 0.704 | — |

Notes: BG-LM = Breusch–Godfrey serial correlation test. JB = Jarque–Bera normality test. ARCH = autoregressive conditional heteroskedasticity test (lag 1). CUSUM = Ploberger–Krämer test based on recursive residuals; "Cross" = whether the statistic exceeds the 95% confidence band at any point. Referenced in Section 4.2.

## References


1. Suski, A.; Remy, T.; Chattopadhyay, D.; Song, C.S.; Jaques, I.; Keskes, T.; Li, Y. Analyzing Electric Vehicle Load Impact on Power Systems: Modeling Analysis and a Case Study for Maldives. *IEEE Access* **2021**, *9*, 125640–125657. [CrossRef]
2. Nogueira, T.; Sousa, E.; Alves, G.R. Electric Vehicles Growth Until 2030: Impact on the Distribution Network Power. *Energy Rep.* **2022**, *8*, 145–152. [CrossRef]
3. Alquthami, T.; Alsubaie, A.; Alkhraijah, M.; Alqahtani, K.; Alshahrani, S.; Anwar, M. Investigating the Impact of Electric Vehicles Demand on the Distribution Network. *Energies* **2022**, *15*, 1180. [CrossRef]
4. Rautiainen, A.; Repo, S.; Jarventausta, P.; Mutanen, A.; Vuorilehto, K.; Jalkanen, K. Statistical Charging Load Modeling of PHEVs in Electricity Distribution Networks Using National Travel Survey Data. *IEEE Trans. Smart Grid* **2012**, *3*, 1650–1659. [CrossRef]
5. Wang, L.; Nian, V.; Li, H.; Yuan, J. Impacts of Electric Vehicle Deployment on the Electricity Sector in a Highly Urbanised Environment. *J. Clean. Prod.* **2021**, *295*, 126386. [CrossRef]
6. Khan, M.O.; Kirmani, S.; Rihan, M. Impact Assessment of Electric Vehicle Charging on Distribution Networks. *Renew. Energy Focus* **2024**, *50*, 100599. [CrossRef]
7. Xiang, Y.; Xue, P.; Wang, Y.; Xu, L.; Ma, W.; Shafie-Khah, M.; Catalao, J.P.S.; Liu, J. Robust Expansion Planning of Electric Vehicle Charging System and Distribution Networks. *CSEE J. Power Energy Syst.* **2023**, *10*, 2457–2469. [CrossRef]
8. Wang, H.; Zhang, X.; Ouyang, M. Energy Consumption of Electric Vehicles Based on Real-World Driving Patterns: A Case Study of Beijing. *Appl. Energy* **2015**, *157*, 710–719. [CrossRef]
9. Wang, R.; Song, Y.; Xu, H.; Li, Y.; Liu, J. Life Cycle Assessment of Energy Consumption and CO2 Emission from HEV, PHEV and BEV for China in the Past, Present and Future. *Energies* **2022**, *15*, 6853. [CrossRef]
10. Jiang, Y.; Meng, D.; Peng, F.; Chen, F.; Li, X.; Song, G. Impacts of Vehicle Electrification on On-Road Energy Consumption Using Real-World Data. *Transp. Res. Part D Transp. Environ.* **2026**, *155*, 105337. [CrossRef]
11. Gay, D.; Rogers, T.; Shirley, R. Small Island Developing States and Their Suitability for Electric Vehicles and Vehicle-to-Grid Services. *Util. Policy* **2018**, *55*, 69–78. [CrossRef]
12. Edoo, M.N.; King, R.T.A. 100% Renewable Energy System for the Island of Mauritius by 2050: A Techno-Economic Study. *Smart Energy* **2025**, *19*, 100199. [CrossRef]
13. Xu, B.; Sharif, A. How Does Transportation Sector Impact Energy Consumption in Macao? Evidence from Wavelet Analysis. *Energy Strategy Rev.* **2025**, *61*, 101875. [CrossRef]
14. Zhang, H.; Tian, M. Shadows of Uncertainty: Unraveling the Impact of Economic Policy Uncertainty on Tourism-Driven Energy Consumption in Macau. *Sustainability* **2025**, *17*, 3716. [CrossRef]
15. Lee, C.C.; Olasehinde-Williams, G.O.; Ibikunle, J.A. An Asymmetric Examination of the Environmental Effect of Tourism in China. *Tour. Econ.* **2022**, *28*, 1872–1887. [CrossRef]
16. Khoi, N.H.; Le, N.H.; Ngoc, B.H. The Effect of Tourism Development on the Ecological Footprint in Singapore: Evidence from Asymmetric ARDL Method. *Curr. Issues Tour.* **2022**, *25*, 2500–2517. [CrossRef]
17. Chishti, M.Z.; Ullah, S.; Ozturk, I.; Usman, A. Examining the Asymmetric Effects of Globalization and Tourism on Pollution Emissions in South Asia. *Environ. Sci. Pollut. Res.* **2020**, *27*, 27721–27737. [CrossRef]
18. Shin, Y.; Yu, B.; Greenwood-Nimmo, M. Modelling Asymmetric Cointegration and Dynamic Multipliers in a Nonlinear ARDL Framework. In *Festschrift in Honor of Peter Schmidt: Econometric Methods and Applications*; Sickles, R., Horrace, W., Eds.; Springer: New York, NY, USA, 2014; pp. 281–314. [CrossRef]
19. Pesaran, M.H.; Shin, Y.; Smith, R.J. Bounds Testing Approaches to the Analysis of Level Relationships. *J. Appl. Econom.* **2001**, *16*, 289–326. [CrossRef]
20. Cai, K.; Sun, C.; Wang, H.; Song, Q.; Wang, C.; Wang, P. The Potential Challenge for the Effective GHG Emissions Mitigation of Urban Energy Consumption: A Case Study of Macau. *Environ. Impact Assess. Rev.* **2022**, *93*, 106717. [CrossRef]
21. Feizi, M.R.; Khodayar, M.E.; Li, J. Data-Driven Distributionally Robust Unbalanced Operation of Distribution Networks with High Penetration of Photovoltaic Generation and Electric Vehicles. *Electr. Power Syst. Res.* **2022**, *210*, 108001. [CrossRef]
22. Flower, I.; Li, F.; Padget, J. Open Data for Modelling the Impacts of Electric Vehicles on UK Distribution Networks: Opportunities for a Digital Spine. *IET Smart Grid* **2024**, *7*, 983–999. [CrossRef]
23. Hao, H.; Cheng, X.; Liu, Z.; Zhao, F. Electric Vehicles for Greenhouse Gas Reduction in China: A Cost-Effectiveness Analysis. *Transp. Res. Part D Transp. Environ.* **2017**, *56*, 68–84. [CrossRef]
24. Parsons, G.R.; Hidrue, M.K.; Kempton, W.; Gardner, M.P. Willingness to Pay for Vehicle-to-Grid (V2G) Electric Vehicles and Their Contract Terms. *Energy Econ.* **2014**, *42*, 313–324. [CrossRef]
25. Song, Q.; Wu, Y.; Li, J.; Wang, Z.; Yu, D.; Duan, H. Well-to-Wheel GHG Emissions and Mitigation Potential from Light-Duty Vehicles in Macau. *Int. J. Life Cycle Assess.* **2018**, *23*, 1916–1927. [CrossRef]
26. Ji, Y.; Zhang, J.; Li, S.; Deng, Y.; Mu, Y. Electric Vehicles Acceptance Capacity Evaluation in Distribution Network Considering Photovoltaics Access. *Energy Rep.* **2023**, *9*, 602–608. [CrossRef]

27. Ahmad, P.; Kumar, S.; Kumar, M.; Singh, N.; Kumar, R.; Singla, M.K. Evaluating the Impact of EV Integration on Distribution Networks Using a Voltage, Reliability, and Power Loss Framework. *Suranaree J. Sci. Technol.* **2026**, *33*, 010407-1. [CrossRef]
28. Sheldon, T.L.; Dua, R. The Dynamic Role of Subsidies in Promoting Global Electric Vehicle Sales. *Transp. Res. Part A Policy Pract.* **2024**, *187*, 104173. [CrossRef]
29. Briseño, H.; Ramirez-Nafarrate, A.; Araz, O.M. A Multivariate Analysis of Hybrid and Electric Vehicles Sales in Mexico. *Socio-Econ. Plan. Sci.* **2021**, *76*, 100957. [CrossRef]
30. Davis, L.W. How Much Are Electric Vehicles Driven? *Appl. Econ. Lett.* **2019**, *26*, 1497–1502. [CrossRef]
31. Shi, X.; Wang, X.; Yang, J.; Sun, Z. Electric Vehicle Transformation in Beijing and the Comparative Eco-Environmental Impacts: A Case Study of Electric and Gasoline Powered Taxis. *J. Clean. Prod.* **2016**, *137*, 449–460. [CrossRef]
32. Yuen, K.H. Cost-Effectiveness Analysis of Electric Vehicles in Singapore. *Singap. Econ. Rev.* **2018**, *63*, 313–338. [CrossRef]
33. Sherafatian-Jahromi, R.; Othman, M.S.; Law, S.H.; Ismail, N.W. Tourism and CO2 Emissions Nexus in Southeast Asia: New Evidence from Panel Estimation. *Environ. Dev. Sustain.* **2017**, *19*, 1407–1423. [CrossRef]
34. Bi, C.; Zeng, J. Nonlinear and Spatial Effects of Tourism on Carbon Emissions in China: A Spatial Econometric Approach. *Int. J. Environ. Res. Public Health* **2019**, *16*, 3353. [CrossRef]
35. Meo, M.; Nathaniel, S.; Shaikh, G.; Kumar, A. Energy Consumption, Institutional Quality and Tourist Arrival in Pakistan: Is the Nexus (a) Symmetric Amidst Structural Breaks? *J. Public Aff.* **2021**, *21*, e2213. [CrossRef]
36. Uzuner, G.; Akadiri, S.S.; Lasisi, T.T. The Asymmetric Relationship Between Globalization, Tourism, CO2 Emissions, and Economic Growth in Turkey: Implications for Environmental Policy Making. *Environ. Sci. Pollut. Res.* **2020**, *27*, 32742–32753. [CrossRef]
37. Wangzhou, K.; Wen, J.J.; Wang, Z.; Wang, H.; Hao, C.; Andlib, Z. Revealing the Nexus Between Tourism Development and CO2 Emissions in Asia: Does Asymmetry Matter? *Environ. Sci. Pollut. Res.* **2022**, *29*, 79016–79024. [CrossRef]
38. Chattopadhyay, M.; Mitra, S.K. Exploring Asymmetric Behavior Pattern from Indian Oil Products Prices Using NARDL and GHSOM Approaches. *Energy Policy* **2015**, *86*, 262–272. [CrossRef]
39. Noumga, J.; Sapnken, F.E.; Kinfack Jeutsa, A.; Tamba, J.G. Asymmetric Impact of Income and Price on Kerosene Consumption in Cameroon: New Evidence from NARDL. *Int. J. Energy Sect. Manag.* **2024**, *18*, 559–576. [CrossRef]
40. Tran, N.D.; Sahu, N.C. Asymmetric Price Response of Industrial Electricity Demand in India. *Util. Policy* **2023**, *82*, 101552. [CrossRef]
41. Kwiatkowski, D.; Phillips, P.C.B.; Schmidt, P.; Shin, Y. Testing the Null Hypothesis of Stationarity Against the Alternative of a Unit Root. *J. Econom.* **1992**, *54*, 159–178. [CrossRef]
42. Newey, W.K.; West, K.D. A Simple, Positive Semi-Definite, Heteroskedasticity and Autocorrelation Consistent Covariance Matrix. *Econometrica* **1987**, *55*, 703–708. [CrossRef]
43. Singh, M.; Yuksel, T.; Michalek, J.J.; Azevedo, I.M. Ensuring Greenhouse Gas Reductions from Electric Vehicles Compared to Hybrid Gasoline Vehicles Requires a Cleaner US Electricity Grid. *Sci. Rep.* **2024**, *14*, 1639. [CrossRef]


**Disclaimer/Publisher's Note:** The statements, opinions and data contained in all publications are solely those of the individual author(s) and contributor(s) and not of MDPI and/or the editor(s). MDPI and/or the editor(s) disclaim responsibility for any injury to people or property resulting from any ideas, methods, instructions or products referred to in the content.